NTIA Report 94-309

Impulse Response Measurements in the 1850-1990 MHz Band in Large Outdoor Cells

J.A. Wepman
J.R. Hoffman
L.H. Loew

U.S. DEPARTMENT OF COMMERCE
Ronald H. Brown, Secretary

Larry Irving, Assistant Secretary
for Communications and Information

JUNE 1994

Product Disclaimer

Certain commercial equipment, instruments, or materials are identified in this paper to specify adequately the technical aspects of the reported results. In no case does such identification imply recommendation or endorsement by the National Telecommunications and Information Administration, nor does it imply that the material or equipment identified is necessarily the best available for the purpose.

CONTENTS

Page

FIGURES vi

TABLES viii

ABSTRACT 1

1. INTRODUCTION 1

2. MEASUREMENT SYSTEM 3
   2.1 Transmitter 3
   2.2 Receiver 3

3. MEASUREMENT PROCEDURE 9

4. MEASUREMENT LOCATIONS 13

5. DATA ANALYSIS METHODS AND RESULTS 17
   5.1 Delay Statistics 18
   5.2 Effects of Spatial Diversity 26
   5.3 Multipath Power Statistics 26
   5.4 Number of Paths, Path Arrival Time, and Path Power Statistics 29
   5.5 Correlation Bandwidth 41

6. SUMMARY AND CONCLUSIONS 46

7. REFERENCES 48

FIGURES

Page

Figure 2.1. Photograph of the measurement system transmitter van 4

Figure 2.2. Photograph of the measurement system receiver van 5

Figure 2.3. Block diagram of the measurement system transmitter 6

Figure 2.4. Block diagram of the measurement system receiver 7

Figure 3.1. Example calibration power delay profile 10

Figure 4.1. Measurement routes in the flat rural cell 14

Figure 4.2. Measurement routes in the hilly rural cell 15

Figure 4.3. Measurement routes in the urban high-rise cell 16

Figure 5.1. Histograms of maximum delay (a), mean delay (b), and RMS delay spread (c) for the flat rural cell using a threshold 20 dB below the peak in each APDP 20

Figure 5.2. Histograms of maximum delay (a), mean delay (b), and RMS delay spread (c) for the hilly rural cell using a threshold 20 dB below the peak in each APDP 21

Figure 5.3. Histograms of maximum delay (a), mean delay (b), and RMS delay spread (c) for the urban high-rise cell using a threshold 20 dB below the peak in each APDP 22

Figure 5.4. Cumulative distributions of maximum delay (a), mean delay (b), and RMS delay spread (c) for the flat rural cell using a threshold 20 dB below the peak in each APDP 23

Figure 5.5. Cumulative distributions of maximum delay (a), mean delay (b), and RMS delay spread (c) for the hilly rural cell using a threshold 20 dB below the peak in each APDP 24

Figure 5.6. Cumulative distributions of maximum delay (a), mean delay (b), and RMS delay spread (c) for the urban high-rise cell using a threshold 20 dB below the peak in each APDP 25

Figure 5.7. Effects of spatial diversity in the flat rural (a), hilly rural (b), and urban high-rise (c) cells 27

FIGURES (cont'd)

Page

Figure 5.8. Average and standard deviation of power (a), peak power (b), and threshold statistics (c) for the flat rural cell 30

Figure 5.9. Average and standard deviation of power (a), peak power (b), and threshold statistics (c) for the hilly rural cell 31

Figure 5.10. Average and standard deviation of power (a), peak power (b), and threshold statistics (c) for the urban high-rise cell 32

Figure 5.11. Cumulative distributions of the number of significant paths for different thresholds for the flat rural (a), hilly rural (b), and urban high-rise (c) cells 34

Figure 5.12. Histograms (a-b) and cumulative distributions (c) of correlation bandwidth for the flat rural cell 42

Figure 5.13. Histograms (a-b) and cumulative distributions (c) of correlation bandwidth for the hilly rural cell 43

Figure 5.14. Histograms (a-b) and cumulative distributions (c) of correlation bandwidth for the urban high-rise cell 44

TABLES

Page

Table 5.1. Mean (μ) and Standard Deviation (σ) of Path Arrival Time (in μs) and Path Power (in dB) Using a -20 dB Threshold for Each Individual Path for APDPs Having a Total of n Paths in the Flat Rural Cell 35

Table 5.2. Mean (μ) and Standard Deviation (σ) of Path Arrival Time (in μs) and Path Power (in dB) Using a -20 dB Threshold for Each Individual Path for APDPs Having a Total of n Paths in the Hilly Rural Cell 36

Table 5.3. Mean (μ) and Standard Deviation (σ) of Path Arrival Time (in μs) and Path Power (in dB) Using a -20 dB Threshold for Each Individual Path for APDPs Having a Total of n Paths in the Urban High-Rise Cell 37

Table 5.4. Mean (μ) and Standard Deviation (σ) of Path Arrival Time (in μs) and Path Power (in dB) Using a -10 dB Threshold for Each Individual Path for APDPs Having a Total of n Paths in the Flat Rural Cell 38

Table 5.5. Mean (μ) and Standard Deviation (σ) of Path Arrival Time (in μs) and Path Power (in dB) Using a -10 dB Threshold for Each Individual Path for APDPs Having a Total of n Paths in the Hilly Rural Cell 39

Table 5.6. Mean (μ) and Standard Deviation (σ) of Path Arrival Time (in μs) and Path Power (in dB) Using a -10 dB Threshold for Each Individual Path for APDPs Having a Total of n Paths in the Urban High-Rise Cell 40

IMPULSE RESPONSE MEASUREMENTS IN THE 1850-1990 MHz BAND IN LARGE OUTDOOR CELLS

Jeffery A. Wepman, J. Randy Hoffman, and Lynette H. Loew*

Mobile impulse response measurements were taken in the 1850-1990 MHz band in three different macrocellular (cell radii of 5 km) environments: flat rural, hilly rural, and urban high-rise. Spatial diversity with a 15-wavelength separation was employed by using a dual-channel receiver. All antennas were omnidirectional and vertically polarized. The data were analyzed to provide delay statistics; spatial diversity statistics; multipath power statistics; number of paths, path arrival time, and path power statistics; and correlation bandwidth statistics. The urban high-rise cell showed more multipath components (out to 4 or 5 μs in delay) than the rural cells. Very long delays (greater than 10 μs), while not seen often, were seen more frequently in the rural cells than in the urban high-rise cell. Parameters to help design a tapped delay model of the radio channel in the different environments are given.

Key words: *arrival time, channel model, coherence bandwidth, correlation bandwidth, impulse response, multipath, power delay profiles, RMS delay spread, spatial diversity, tapped delay model, wideband measurements*

1. INTRODUCTION

The impulse response of the radio propagation channel is of great importance in the design, development, and planning of radio systems since it completely describes the radio propagation channel. Once the impulse response of a channel is known, the actual received signal can be determined given a specific transmitted signal by convolving the transmitted signal with the impulse response. Modelling of the impulse response has been and will continue to be an important effort, as will be hardware and software simulation utilizing impulse responses. Additionally, there have been many attempts made throughout the years to correlate the performance of radio systems through a propagation channel using analytical methods with measured impulse responses. Impulse response measurements are therefore needed to support the ongoing channel modelling and simulation efforts as well as to support analytical methods required in the development of new telecommunication services such as Personal Communication Services (PCS) and advanced cellular mobile systems. This paper addresses this need by discussing a set of impulse response measurements taken in the 1850-1990 MHz band.**

---

* The authors are with the Institute for Telecommunication Sciences, National Telecommunications and Information Administration, U.S. Department of Commerce, Boulder, CO 80303

** Funding for these measurements was provided by Telesis Technologies Laboratory, Inc.

The impulse response measurements presented in this paper were taken in three different cell environments in the Denver, Colorado, area. These environments included a flat rural cell, a hilly rural cell, and an urban high-rise cell. The measurements within each cell were made using a fixed-location receiver placed at the center of the cell and a mobile transmitter installed in a measurement van. All of the measurements were made within a 5-km radius of the center of each cell, using omnidirectional, vertically polarized transmit and receive antennas. Impulse response data were collected as the transmitter van travelled along predetermined routes within each cell. The data were analyzed to provide delay statistics; spatial diversity statistics; multipath power statistics; number of paths, path arrival time, and path power statistics; and correlation bandwidth statistics.

2. MEASUREMENT SYSTEM

The impulse response measurements presented in this report were taken using the Digital Impulse Response Measurement System (patent pending) developed jointly by the Institute for Telecommunication Sciences and Telesis Technologies Laboratory, Inc. This system is comprised of a separate transmitter and a dual-channel receiver employing spatial diversity. The transmitter was installed in a mini-van and utilized a well-regulated diesel generator mounted on a trailer to provide AC power. Figure 2.1 shows a photograph of the transmitter van. For the measurements in both of the rural cells, the receiver was mounted in a large van and kept at a fixed location. The antennas were mounted on a telescoping mast 8.7 m aboveground. A photograph of the receiver van is shown in Figure 2.2. In the urban high-rise cell, the receiver was located on the rooftop of a building approximately 103 m aboveground in the center of the high-rise district in downtown Denver. The building height was typical for the buildings in this area. The height of the ground above average terrain at the receiver site out 5 km in radius was -4 m, +12 m, and -8 m in the flat rural, hilly rural, and urban high-rise cells, respectively. These heights do not include the antenna mast heights in the rural cells or the building height in the urban high-rise cell.

2.1 Transmitter

A block diagram of the transmitter is shown in Figure 2.3. The pseudo-random noise (PN) code generator produces a 511-bit maximal-length code and is clocked at a 10 Mbit/s rate by a rubidium frequency standard. The PN code is then level-shifted to eliminate the DC component and amplitude clamped. A low-pass filter with a cutoff frequency of 10 MHz is used to attenuate spectral components above the first null. This PN code is used to modulate an RF carrier in the 1850-1990 MHz band producing a binary phase-shift keyed (BPSK) signal. This signal is bandpass filtered, amplified to the appropriate level, and transmitted through a vertically polarized, omnidirectional, biconical antenna with a gain of 0 dBi. The power level is set to provide 50 W effective isotropically radiated power (EIRP).

2.2 Receiver

Figure 2.4 shows the receiver block diagram. A personal computer is used to control the measurement system receiver via a GPIB bus. The spectrum analyzers and digital oscilloscope are all under GPIB control. A vertically polarized, omnidirectional, biconical antenna with a gain of 0 dBi is used for each channel to receive the transmitted signal. The spatial separation between the antenna for Channel 1 and the antenna for Channel 2 is 15 wavelengths at the center of the 1850-1990 MHz band. The received signal is first bandpass filtered to eliminate undesired signals and then amplified using low-noise amplifiers to minimize the system noise figure. After filtering and amplification, the BPSK signal is downconverted to IF using portable spectrum analyzers and an additional double-balanced mixer stage. The IF signal is then low-pass filtered to eliminate the local oscillator frequency from the additional mixer stage. After this, video amplifiers are used to boost the signal level before it is digitized by the digital oscilloscope. A rubidium frequency standard is used to phase lock the spectrum analyzers and the signal generators. The divide-by-511 counter is clocked by the 10-MHz output from the

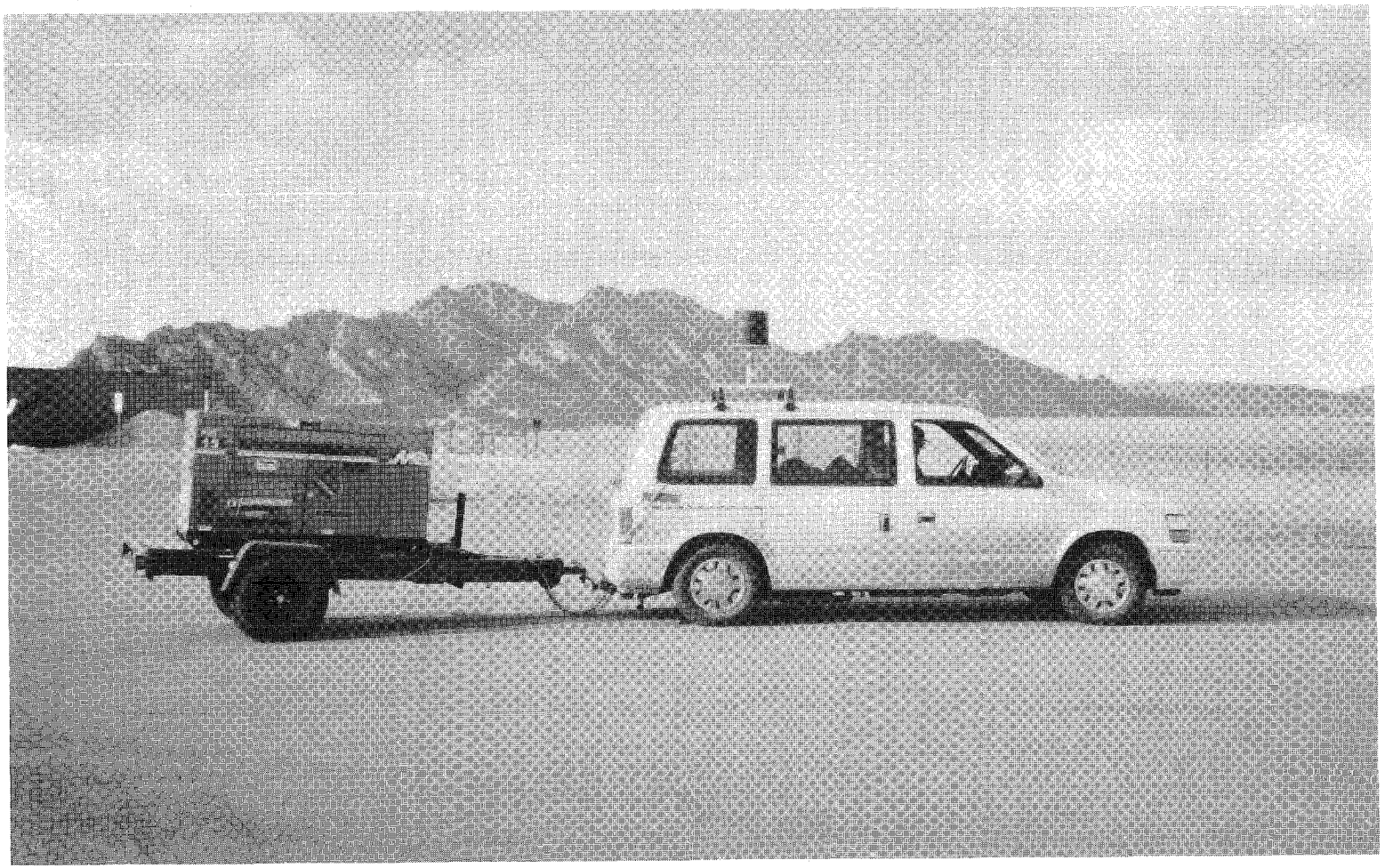

Figure 2.1. Photograph of the measurement system transmitter van.

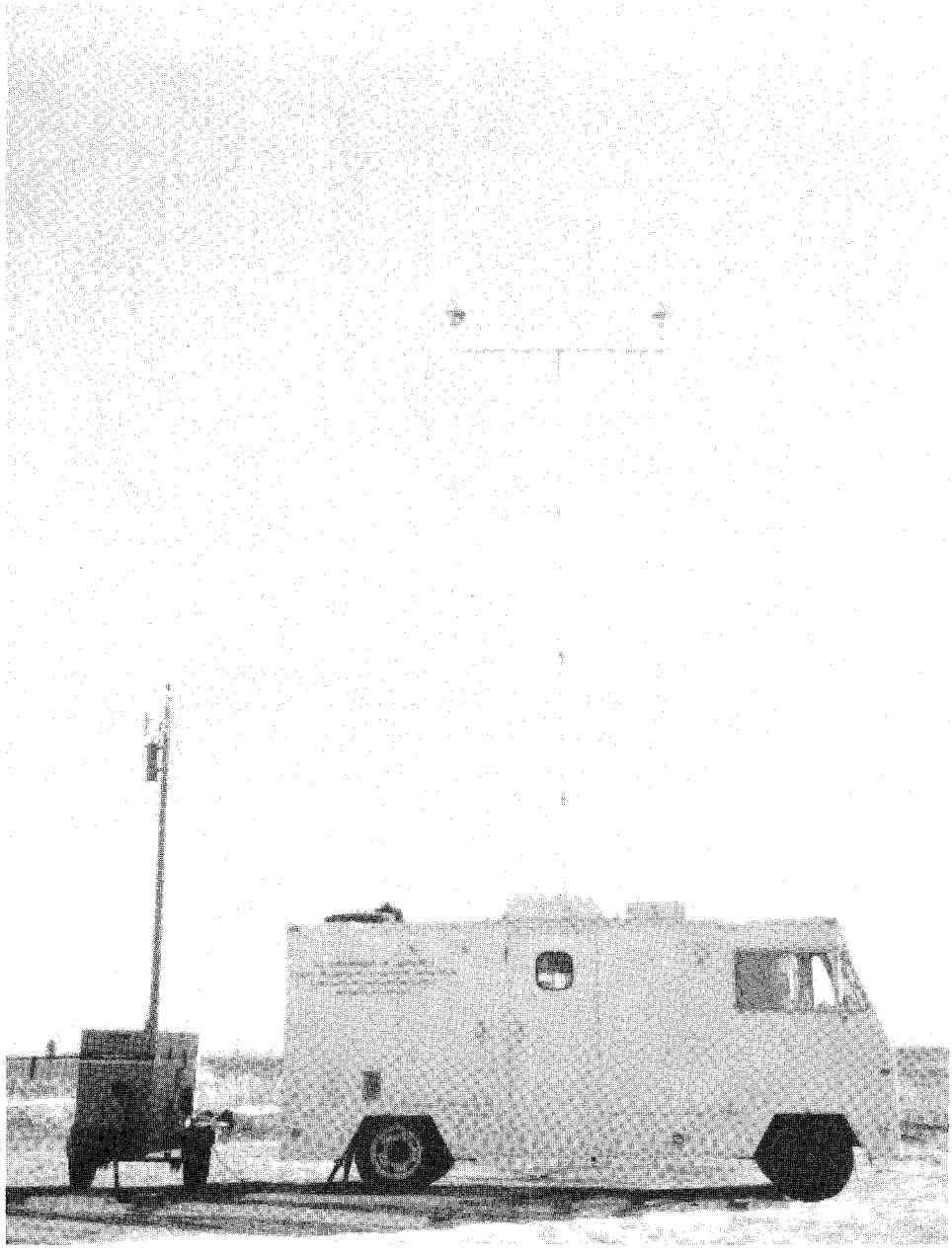

Figure 2.2. Photograph of the measurement system receiver van.

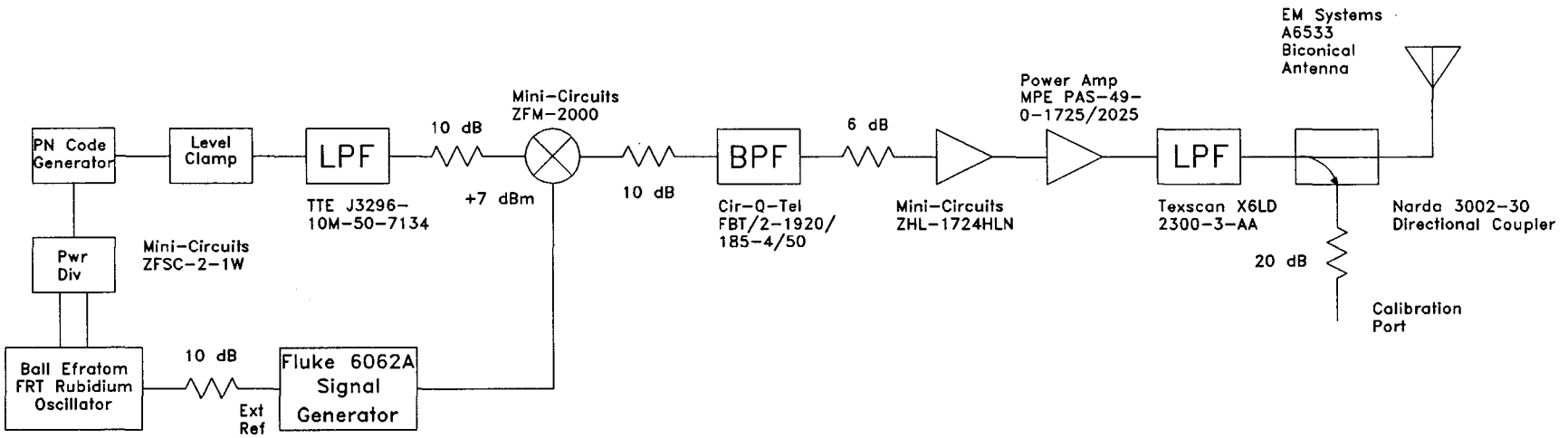

Figure 2.3. Block diagram of the measurement system transmitter.

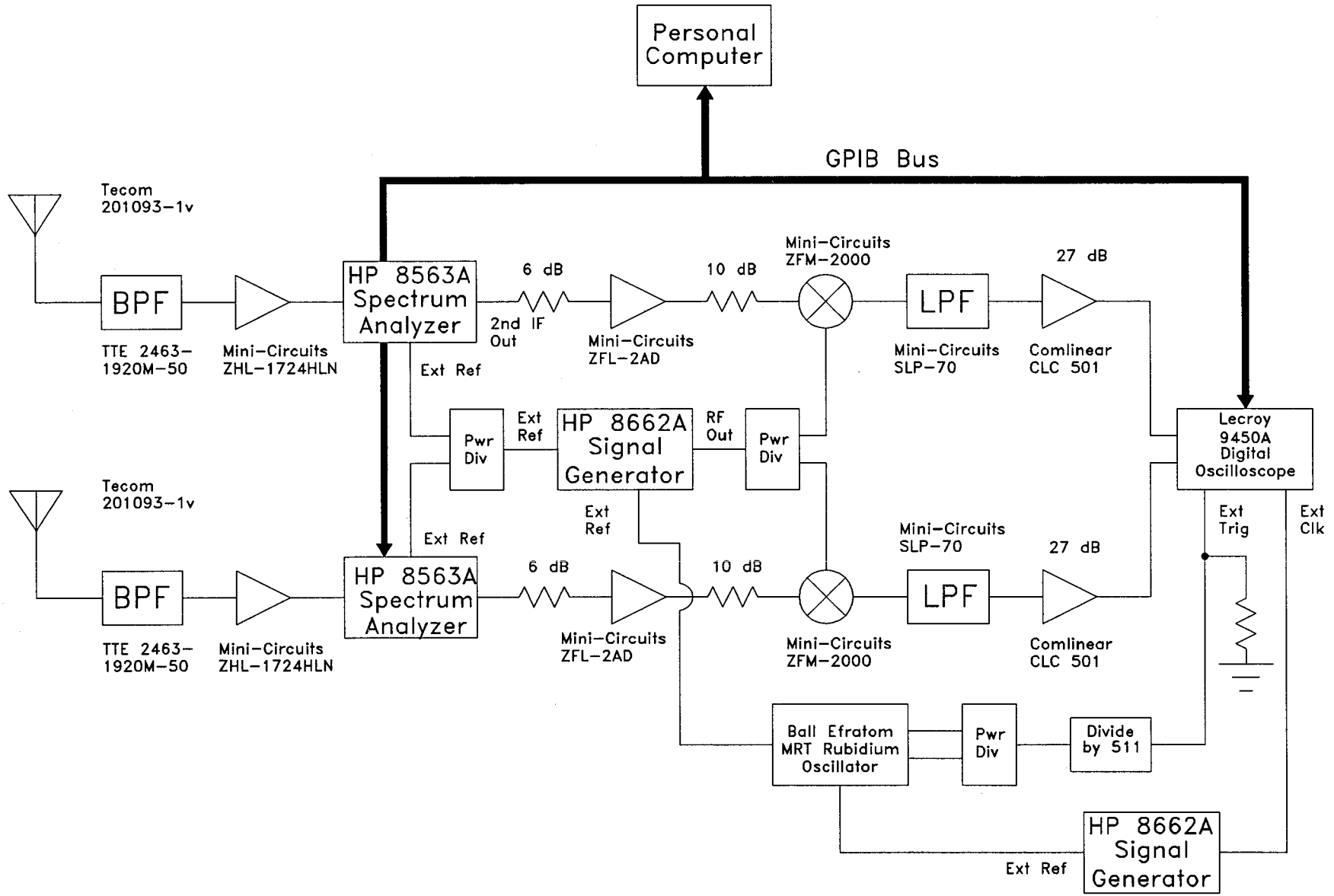

Figure 2.4. Block diagram of the measurement system receiver.

rubidium frequency standard. The output of this counter produces a pulse train used for externally triggering the digital oscilloscope. The pulses (100-ns pulse width) occur at the start of every PN code word transmitted. Synchronization between the PN code word and this pulse train is accomplished by circuitry that resets both the PN code generator in the transmitter and the divide-by-511 counter in the receiver simultaneously. This synchronization provides absolute time measurement capability to the Digital Impulse Response Measurement System. The absolute time capability has a resolution determined by the relative frequency drift between the transmitter and receiver frequency standards.

After the signal is digitized by the oscilloscope, the digitized IF signal is then transferred over the GPIB bus to the computer and stored on the hard disk. The in-phase and quadrature phase components, as well as the impulse responses, are derived in software; this processing can be performed either immediately after the raw data has been taken or at a later date.

3. MEASUREMENT PROCEDURE

The calibration, system verification, and setup procedures described here were performed in each cell every morning before measurements began. Measurements were made during the daytime from approximately 8 AM to 5 PM. Before calibration began, the transmitter and receiver equipment were warmed up for one-half hour. The rubidium frequency standards were warmed up for at least 24 hours prior to calibration. The output power of the transmitter into a 50-ohm load was measured and recorded using a directional coupler and a power meter. Three primary calibration procedures were performed: frequency calibration, amplitude calibration, and absolute time calibration.

The frequency calibration procedure consisted of tuning the rubidium frequency standard located in the receiver so that its frequency matched that of the rubidium frequency standard located in the transmitter. This was accomplished by connecting the 5-MHz outputs of each frequency standard to a gain/phase meter and adjusting the frequency of the receiver's frequency standard to minimize the change in the phase difference over time between the two frequency standards. Frequency calibration was performed and highly stable rubidium frequency standards were used for three primary reasons. First, it was necessary to ensure that the in-phase and quadrature phase components for an individual impulse response did not rotate appreciably during data collection. Secondly, the sampling clock had to be accurate enough to ensure that the correct number of samples were taken within the 511-bit PN code word. If this condition is not met, the correlation noise floor increases, thereby decreasing the interval of discrimination (ID). The ID is the amplitude difference between the correlation peak and the peak of the noise in the power delay profile (PDP). The PDP is the magnitude squared of the measured complex impulse response. Finally, the absolute time capability required that the PN code generator in the transmitter and divide-by-511 board in the receiver remained synchronized as closely as possible for the entire duration of the measurements. Therefore, the rubidium frequency standards were used to clock both the PN code generator and the divide-by-511 board.

The second type of system calibration that was performed was a receiver amplitude calibration. This entailed connecting the transmitter directly to the receiver via a coaxial cable, with a variable attenuator inserted between the transmitter and receiver to control the amplitude of the signal input into the receiver. A complete amplitude calibration was performed after configuration of the measurement system before the actual measurements commenced. The complete amplitude calibration provided a series of PDPs at varying RF input power levels to the receiver for both receiver channels. The RF input power was decreased in 10-dB steps from the receiver's 0.5-dB compression point until the signal-to-noise ratio was so low that no PDP could be obtained.

An example of these calibration PDPs for a high-level input signal into the receiver (-48 dBm) is shown in Figure 3.1. From this PDP, the ID is seen to be approximately 51 dB. This approaches the theoretical limit of a 9-bit PN code generator given by $20*\log_{10}(2^n-1) \approx 54$ dB where $n = 9$. From the calibration PDPs, it is noted that as the RF input power into the receiver decreases to roughly -60 dBm, the ID does not decrease. As the RF input power into the receiver decreases below -60 dBm, the ID decreases due to system noise. Processing gain is the difference between the output and input signal-to-noise ratios of a system [1]. The processing gain from a 9-bit PN code generator is given as $10*\log_{10}(2^n-1) \approx 27$ dB. This

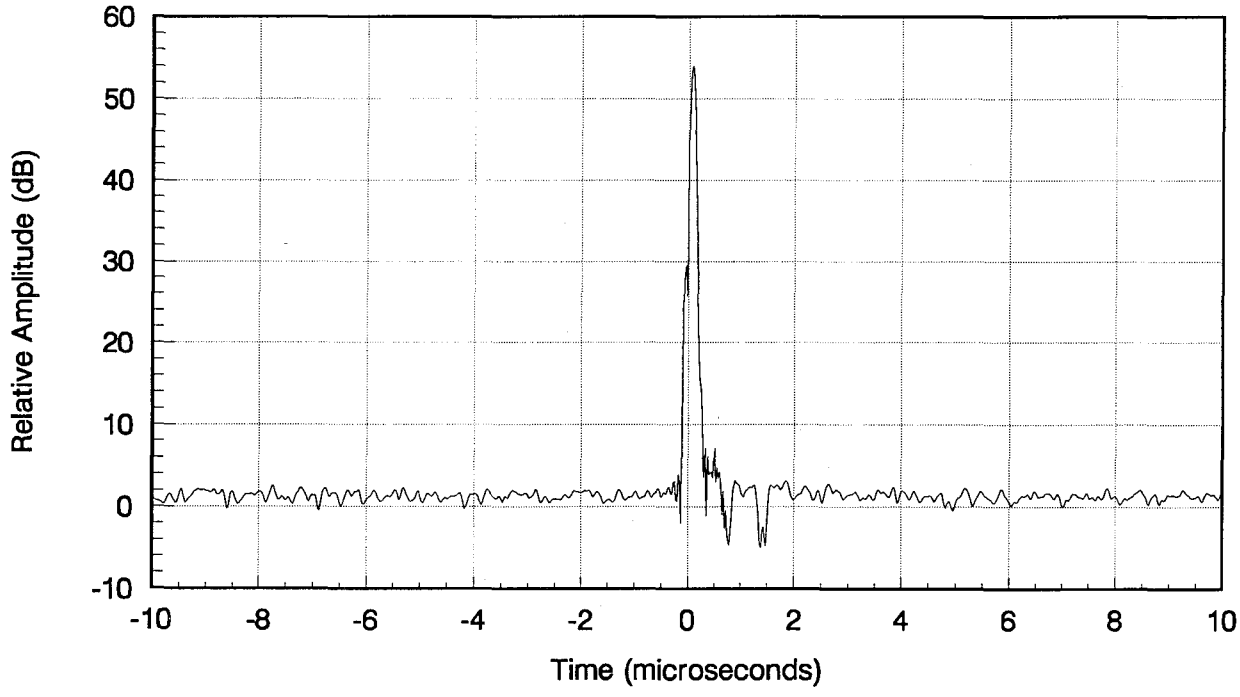

Figure 3.1. Example calibration power delay profile.

means that when the RF input power into the receiver is equal to the system noise of the receiver, the correlation peak will be 30 dB above the average noise level. This occurs when the RF input power is approximately -91 dBm. The presence of multipath even further reduces the ID.

The complete amplitude calibration is important since it allows verification of the proper operation of the measurement system, provides a relationship between the received signal power and the PDP, and allows approximate determination of the receiver noise figure from the PDP.

Every morning before measurements were made, an abbreviated amplitude calibration was performed. This procedure was identical to the complete amplitude calibration procedure except that the RF input power to the receiver was limited to one high and one low level. The PDPs obtained using these input power levels into the receiver were then compared to the corresponding PDPs generated in the complete calibration procedure. The results of this comparison showed whether the measurement system was operating properly.

The absolute time calibration was then performed. This procedure required a reset cable to be connected between the transmitter and receiver. A single switch then reset both the PN code generator in the transmitter and the divide-by-511 board in the receiver simultaneously. This ensured that the PN code and the external trigger pulse to the digital oscilloscope were synchronized within a few nanoseconds. The reset cable was then disconnected. With the transmitter still connected to the receiver via the coaxial cable and attenuator, data were captured at a high-level RF input signal into the receiver. The PDP was obtained and the time that the peak of the PDP occurred was recorded. If there was no delay through the transmitter and

receiver systems and the cable connecting the two, the peak of the PDP would occur at time zero. Due to delays through the filters and other components in the transmitter and receiver, however, the peak received signal occurred at about 300 ns.

After all of the calibration procedures were completed, the radio frequency spectrum was observed to determine the potential interfering signals in or near the measurement frequency band. The transmitter was disconnected and turned off while the receiver inputs were connected to the receive antennas. The antennas were mounted on the top of the telescoping mast for the rural sites and on top of the building in the urban high-rise cell. The receiver spectrum analyzers were set up in sweep mode to observe and display frequencies from 1850 to 1990 MHz. Interfering signals at several different frequencies were seen within the band in all of the cells. The center frequency of the measurement system was set such that any interference from or to existing services would be avoided.

An over-the-air test, which was primarily qualitative in nature, was then performed to test the proper functioning of the entire transmitter/receiver measurement system including the antennas and antenna feed cables. For this test, the transmitter was separated from the receiver by approximately 0.15 km. The transmitter was turned on and the received signals on both channels were checked for proper frequency and amplitude. Data were captured for both channels and the corresponding PDPs were compared to expected results to determine if the entire system was operating properly. The transmitter was kept operating while the rest of the setup procedures were performed and was not turned off until the measurements in that cell were completed for the day.

The transmitter van was moved to the beginning of the first route selected for measurement within the cell. The data acquisition and control software was activated at the receiver to prepare the measurement system for data collection. First, under computer control, the receiver hardware was initialized. Based upon the received signal levels, the amplitude sensitivity of both channels of the digital oscilloscope was automatically set by an autoscaling procedure. The sensitivity of each channel was set independently. The system operator had the option of overriding the automatic amplitude sensitivity settings and entering those desired. The system operator was then prompted for information to be stored in the data file header. This information included the cell number and description; the route number within the cell; and the transmit antenna type, polarization, and height.

After these setup procedures, the data acquisition was initiated and the transmitter van began travelling along the selected route. A rapid succession of 10 PDPs was taken at intervals of approximately 0.7 s as the transmitter van was moving. Within this succession of PDPs a time interval of 255.5 μs (5 times the PN code word duration) was used between the beginning of one impulse and the beginning of the next. Spatial distance between each PDP within the succession of 10 ranged from approximately 0.17 to 0.63 cm. The spatial distance between each succession of 10 PDPs ranged from 4.66 to 17.26 m. When the transmitter had to stop along the measurement routes, the data collection was suspended. The control software monitored signal levels on both channels and if either signal level was too low or too high for adequate digitization, an alarm would sound and the corresponding data on both channels would not be recorded. If the signal levels were persistently too low or too high, the measurement van was stopped and the autoscale procedure was executed again before restarting data acquisition. Data

of appropriate signal level were stored on the computer hard disk. Periodically, while data were not being collected, the previously recorded data would be spot checked by looking at randomly chosen PDPs. After all of the data had been acquired for the day, the data were checked by looking at selected PDPs taken that day. Assured that the data were sound, the data were backed up onto optical disk.

4. MEASUREMENT LOCATIONS

The measurements were taken in three different cell environments: flat rural, hilly rural, and urban high-rise. The flat rural area consisted primarily of open spaces and farmland. The receiver was located at the center of the cell along Route 256 east of the intersection with Road 35 between the towns of Gilcrest and La Salle, Colorado. This site was approximately 45 km east of the foothills of the Rocky Mountains. Throughout most of the cell, the elevation varied by only about 30 m. There were some small hills in the far southeast corner of the cell with elevations up to 80 m above the receiver site. Figure 4.1 shows a map of this cell; the measurement routes followed by the transmitter are marked on this map.

The hilly rural area consisted primarily of open space areas with some valleys and rolling hills. The receiver was located at the U.S. Department of Energy Wind Site off of Highway 128 between Boulder and Golden, Colorado. The elevation varied by about 300 m throughout this cell. The foothills of the Rocky Mountains were approximately 5 km west of the receiver site. A map of this cell showing the measurement routes taken by the transmitter van is shown in Figure 4.2.

Figure 4.3 shows a map of the urban high-rise cell, with the routes marked where the transmitter van travelled. The receiver was located on the top of a building 103 m aboveground at 410 17th St. in the center of the high-rise district in Denver, Colorado. This area consists of closely spaced buildings with heights typically ranging from 25 to 35 stories. The elevation of the terrain throughout this cell varied by about 85 m.

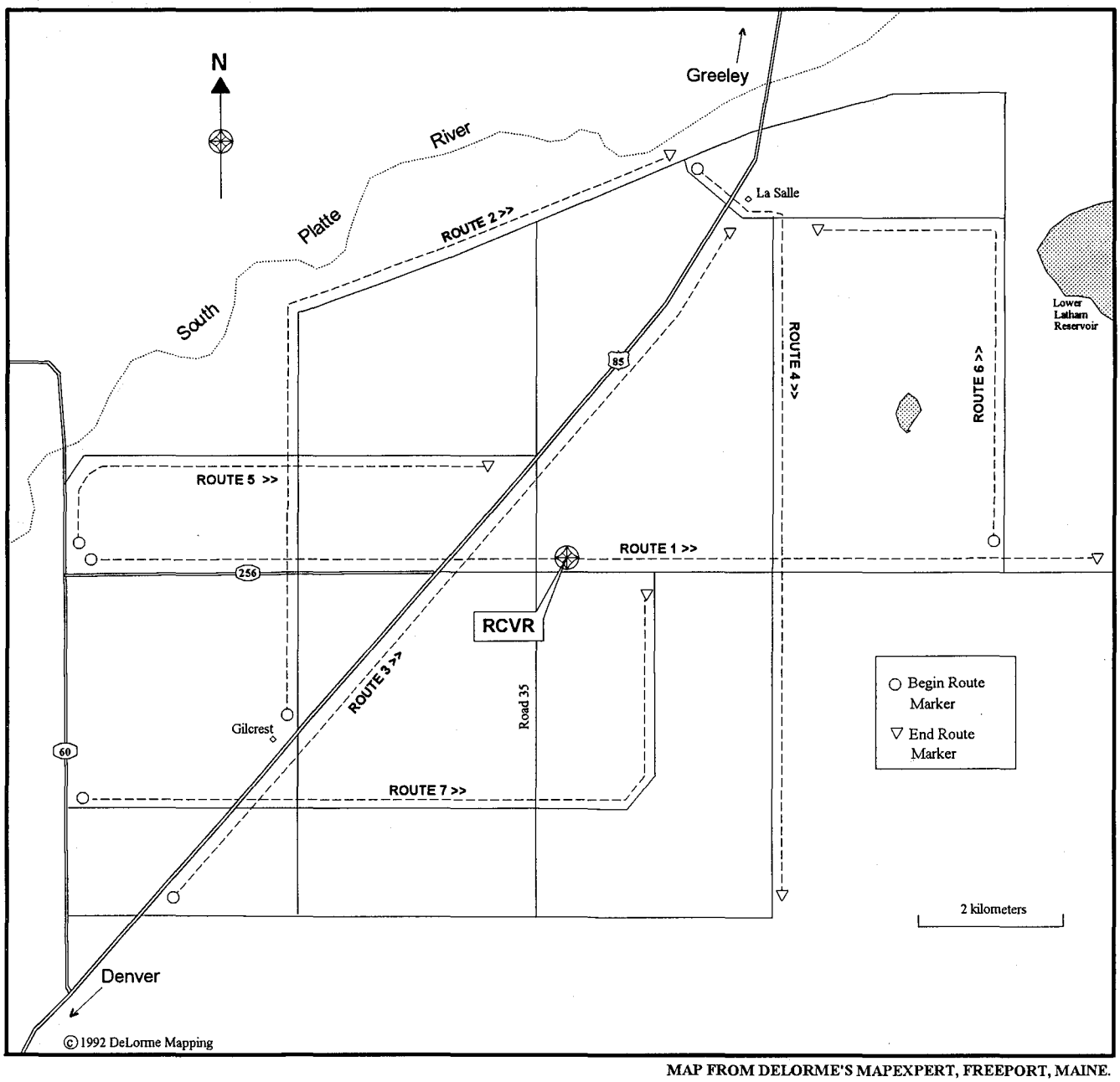

MAP FROM DELORME'S MAPEXPERT, FREEPORT, MAINE.

Figure 4.1. Measurement routes in the flat rural cell.

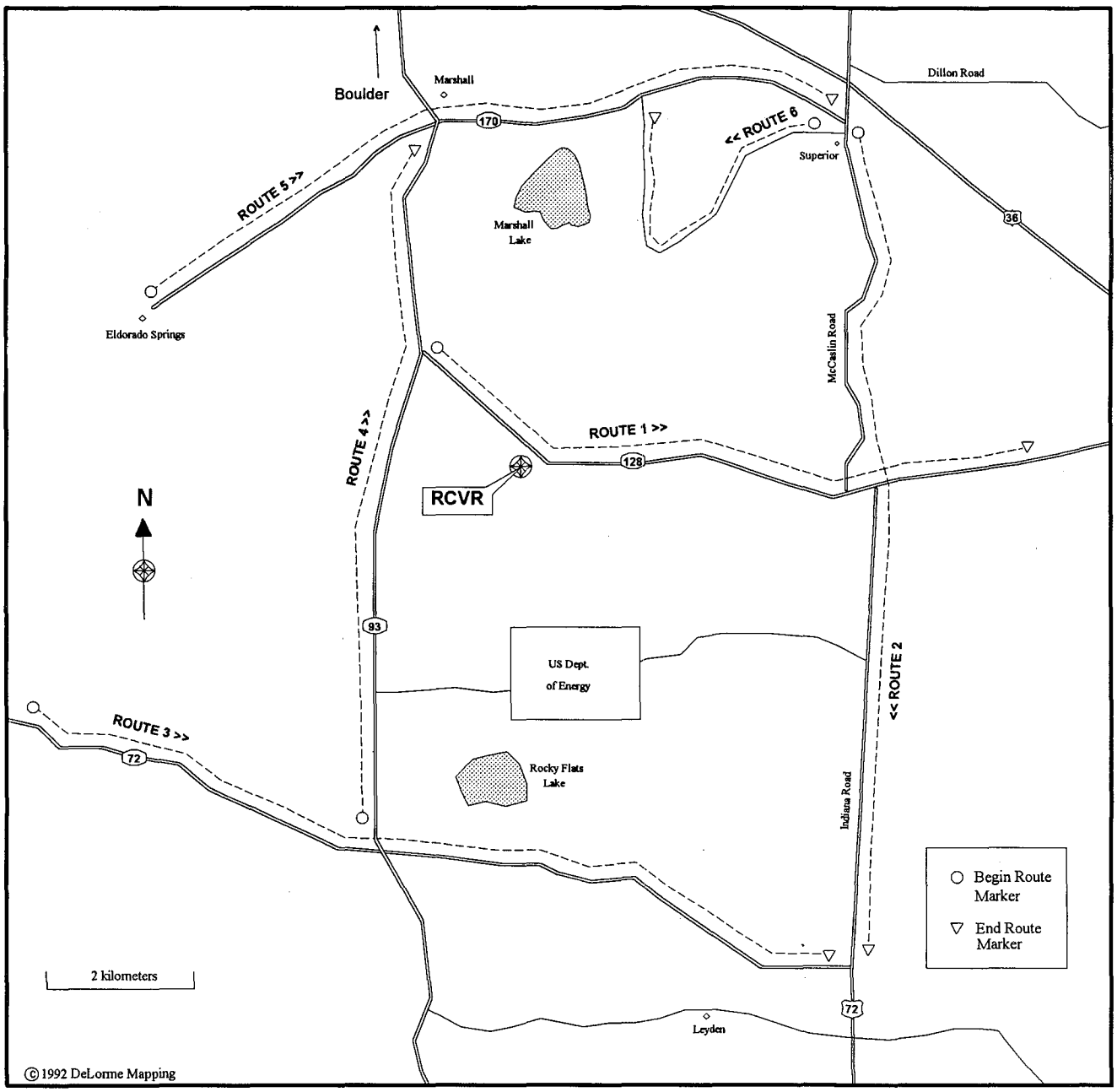

MAP FROM DELORME'S MAPEXPERT, FREEPORT, MAINE.

Figure 4.2. Measurement routes in the hilly rural cell.

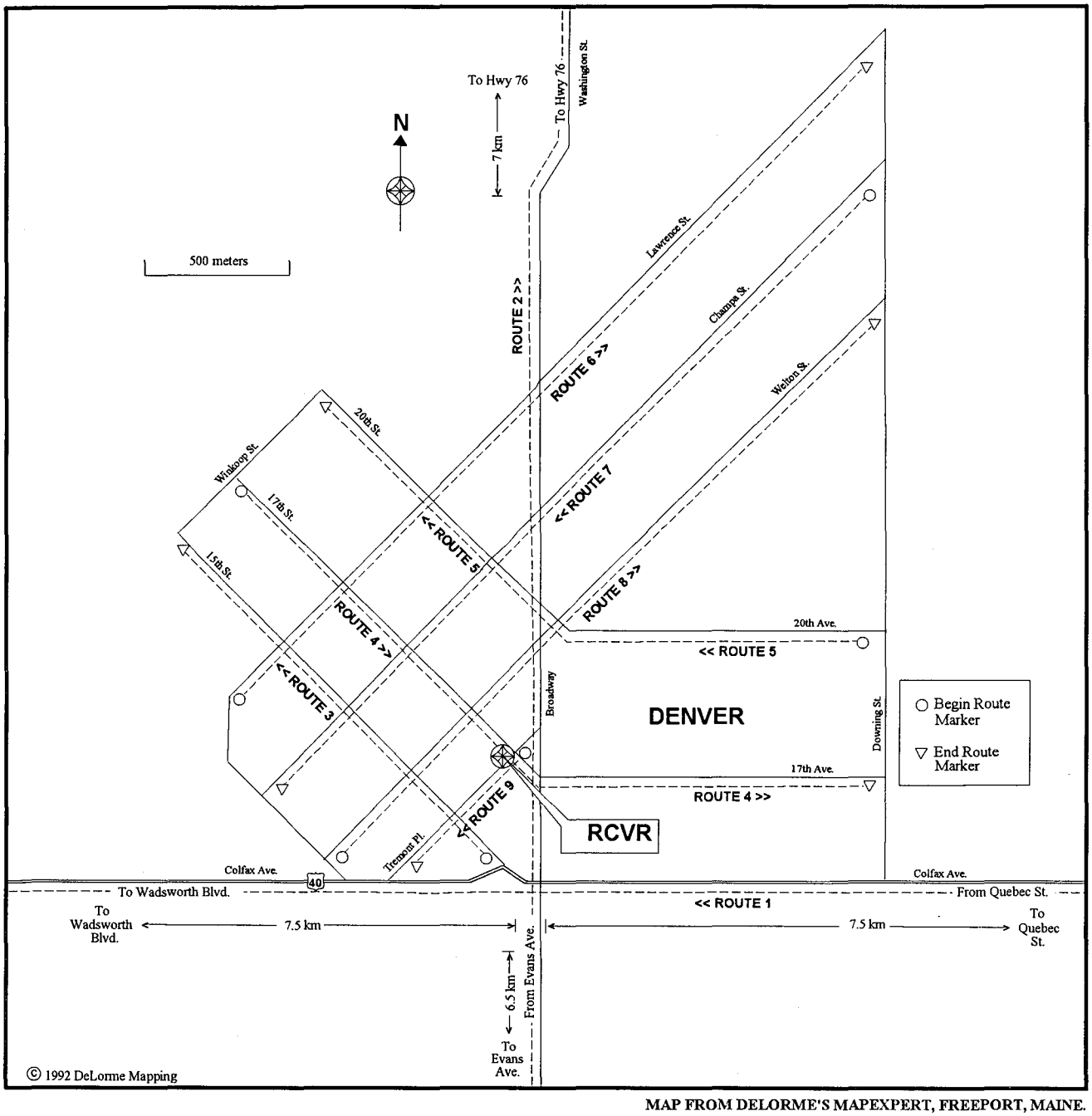

MAP FROM DELORME'S MAPEXPERT, FREEPORT, MAINE.

Figure 4.3. Measurement routes in the urban high-rise cell.

5. DATA ANALYSIS METHODS AND RESULTS

This section provides a detailed explanation of how the data were analyzed, along with a presentation of the results. The general types of analyses presented may be classified as delay statistics, number of paths and arrival time statistics, multipath power statistics, correlation bandwidth statistics, and spatial diversity statistics. The statistics were formed from data taken in each cell separately. All statistics were computed using the data from Channel 1 only, except for the spatial diversity statistics which inherently rely on the data from both channels. All of the raw data were taken utilizing the absolute time circuitry. Synchronization was lost for the data taken in the urban high-rise cell, so that set of data does not have the absolute time information. The results of the data analysis presented in this paper did not make use of the absolute time information so that previously written analysis software could be used. All of the statistics were computed from averaged PDPs (APDPs). Therefore, the first step in the data analysis process, common to all of the statistics, was to develop the APDPs.

An APDP was calculated from each succession of 10 PDPs according to the following procedure. Initially, the total signal power was determined for each of the 10 PDPs and the PDP with the greatest total power was identified. Any of the 10 PDPs with a total power 10 dB or more below the PDP with the greatest total power was tagged as invalid and excluded from processing. Therefore, a set of valid PDPs within the succession of 10 PDPs consisted of one to ten PDPs. Usually, there were 10 PDPs within a set of valid PDPs.

In order to compute an APDP, alignment in time between all valid PDPs (within a succession of 10 PDPs) was required. Alignment was accomplished by performing cross correlations between consecutive valid PDPs. The second valid PDP was aligned with the first valid PDP by shifting the second one in time according to the results of the correlation. Each subsequent valid PDP was then aligned with the previous (aligned) valid PDP. Once aligned, all of the valid PDPs (within the succession of 10 PDPs) were averaged together to give an APDP. This type of alignment was utilized to obtain average values of power for signals with the same delay time.

The received signal levels obtained in the measurements tended to be relatively low in some locations due to the long distances between the transmitter and receiver, limited transmitter power as required by the experimental license, and shadow fading. Due to these relatively low signal levels and the presence of multipath, an ID of only 20 dB could be guaranteed from APDPs taken in these locations. Because of this and also to treat APDPs of varying IDs on an equivalent basis, only delayed signals within 20 dB of the peak value in the APDP were counted as significant for the computations. The APDPs were used as the basis for computing all of the statistics.

To ensure that noise was not included in the statistical computations, an APDP was only considered valid (for inclusion in the statistics) if its ID was 23 dB or greater. This assured that samples of the APDP up to 20 dB below the peak received signal would be actual delayed signals and not noise (by providing a 3-dB buffer between the peak of the noise and the region where the amplitude of delayed signals was considered significant). If the APDP had an ID less than 23 dB, this APDP, as well as the APDP that was computed from PDPs taken simultaneously on the other channel, were not counted in the statistics. This was done so that every APDP from one channel had a corresponding APDP (computed from PDPs taken simultaneously on the other channel) as required for the spatial diversity processing.

Alignment in time between each APDP was then addressed. All of the valid APDPs (i.e., those APDPs having at least one sample 23 dB or more above the peak noise value and having the corresponding APDP on the other channel also meet this criterion) were then shifted in time such that the first perceptible received copy of the transmitted signal was set to zero time. After this alignment procedure, the APDPs were ready to be utilized in the statistical computations. Note that when the term APDP is used in the rest of this paper, that it implies a valid and aligned APDP.

In the discussion of the various different statistics that follows, the number of valid APDPs within each cell should be kept in mind. The flat rural cell had 3220 valid APDPs, the hilly rural cell had 1341 valid APDPs, and the urban high-rise cell had 3813 valid APDPs. The relatively low number of valid APDPs in the hilly rural cell is indicative of the terrain. In many locations within the cell, the signal level was too low to guarantee a sufficient ID. This was probably due to shadow fading caused by the hills.

5.1 Delay Statistics

The three types of delay statistics that were analyzed were maximum delay, average delay, and RMS delay spread. Each of these parameters is a single number that is used to describe an entire APDP. Therefore, these parameters are useful in statistically describing a set of many impulses. For the computation of these parameters, since delayed signals within 20 dB of the peak value in the APDP are the only ones counted as significant, samples within each APDP that are more than 20 dB below the maximum signal level are set to zero.

The maximum delay p is found for each APDP by finding the delay time between the first and last perceptible reception of the transmitted signal in the APDP. The average delay d (in s) is the average of the power-weighted delays (with respect to the time-of-arrival of the first perceptible reception of the transmitted signal) in the APDP. This average delay is given as [2-4]

$$d = \frac{\sum_{k=1}^{N} \tau_k \, P(\tau_k)}{\sum_{k=1}^{N} P(\tau_k)}$$

where N is the number of sample data points in the APDP, τ_k is the time delay (in s) of the k^{th} sample in the APDP relative to the time of occurrence of the first perceptible reception of the transmitted signal, and $P(\tau_k)$ is the value of the APDP at a time delay of τ_k.

While the average delay is the average of the power-weighted delays in the APDP, RMS delay spread is the standard deviation of the power-weighted delays [5]. The RMS delay spread is computed for each APDP by [2-4]

$$S = \left[\frac{\sum_{k=1}^{N} (\tau_k - d)^2 \, P(\tau_k)}{\sum_{k=1}^{N} P(\tau_k)} \right]^{\frac{1}{2}} .$$

For each cell, a histogram and cumulative distribution of the maximum delay, average delay, and RMS delay spread are computed.

Figures 5.1a-5.3a show the histograms for the maximum delay for the flat rural, hilly rural, and urban high-rise cells, respectively. These histograms show the number of APDPs having maximum delay values that fall within 0.5-μs bins. The flat rural cell has a distribution such that maximum delays less than 1 μs occur most frequently. As the maximum delay increases beyond 1 μs, the number of APDPs per bin decreases rapidly. The hilly rural cell has a similar distribution with maximum delays less than 0.5 μs occurring most frequently. The distribution of maximum delays is much wider for the urban high-rise cell (than in the rural cells) with maximum delays occurring most frequently around 3 to 4 μs.

Figures 5.1(b-c)-5.3(b-c) show the histograms for the mean delay and RMS delay spread for the flat rural, hilly rural, and urban high-rise cells, respectively. These histograms show the number of APDPs having mean and RMS delay spread values that fall within 0.1-μs bins. The distributions between the two rural cells for both mean delay and RMS delay spread are relatively similar. Mean delays between 0.1 and 0.2 μs occur most frequently in both of the rural cells. As the mean delay increases above 0.2 μs, the number of APDPs per bin decreases rapidly. RMS delay spread values of up to 0.2 μs occur most frequently in the flat rural cell, whereas in the hilly rural cell, RMS delay spread values of up to 0.1 μs occur most frequently.

The mean delays in the urban high-rise cell show a wide and fairly even distribution from 0.1 to 1.4 μs before slowly tapering off. The RMS delay spread distribution shows a more or less bell shaped distribution with the maximum number of APDPs having values from 0.6 to 0.9 μs.

The cumulative distributions of maximum delay, mean delay, and RMS delay spread are given for the flat rural, hilly rural, and urban high-rise cells in Figures 5.4-5.6, respectively. By comparing the cumulative distributions from both rural cells, it is evident that the probability of exceeding the maximum delay, mean delay, and RMS delay spread is slightly lower for the flat rural cell than for the hilly rural cell. This suggests that there was slightly more multipath present during the measurements in the hilly rural cell than in the flat rural cell.

The cumulative distribution of maximum delay for the urban high-rise cell shows a much higher probability of exceeding maximum delay values than in the rural cells in the range up to about 5 μs (Figures 5.4a-5.6a). As an example, the probability of exceeding a maximum delay of 4 μs is about 0.45 for the urban high-rise cell and only 0.12 for the flat rural cell. Beyond 10 μs, the cumulative distribution of maximum delay for the urban high-rise cell shows a lower probability of exceeding the maximum delay values than in the rural cells. This suggests that very long delays (greater than 10 μs), while not seen often, were seen more frequently in the rural cells than in the urban high-rise cell.

Compare the cumulative distribution of mean delay between the urban high-rise cell and the rural cells (Figures 5.4b-5.6b). Up to 1.5 μs, the probability of exceeding the mean delay is much greater for the urban high-rise cell than for the rural cells. Similarly, the cumulative distribution of RMS delay spread shows a higher probability of exceeding RMS delay spread values (up to 1 μs) in the urban high-rise cell than in the rural cells (Figures 5.4c-5.6c). The histograms and cumulative distributions of maximum delay, mean delay, and RMS delay spread indicate that, although very long delays are seen more frequently in the rural cells, there are significantly more delayed signals (out to 5 or 6 μs) with higher power in the urban high-rise cell than in the rural cells.

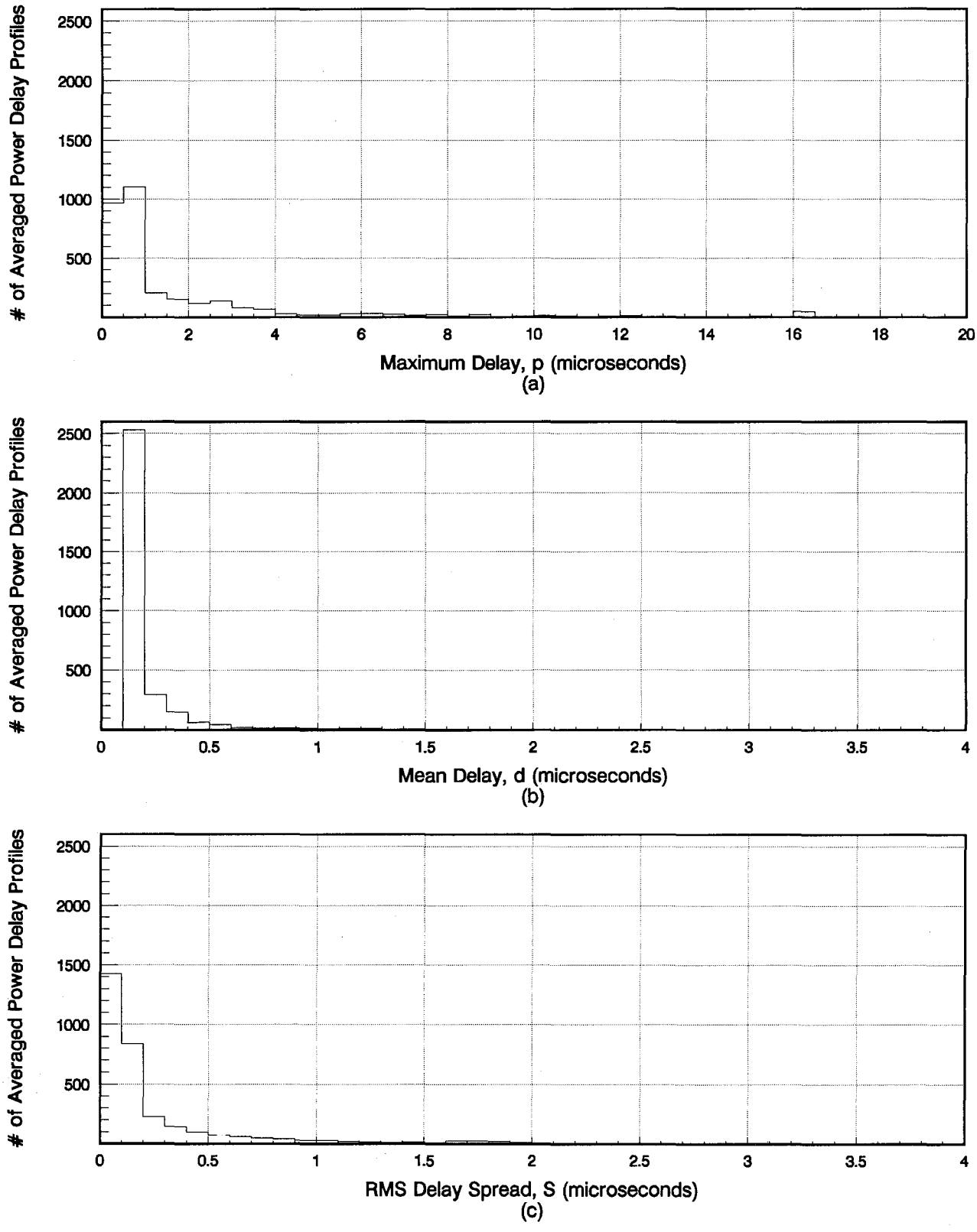

Figure 5.1. Histograms of maximum delay (a), mean delay (b), and RMS delay spread (c) for the flat rural cell using a threshold 20 dB below the peak in each APDP.

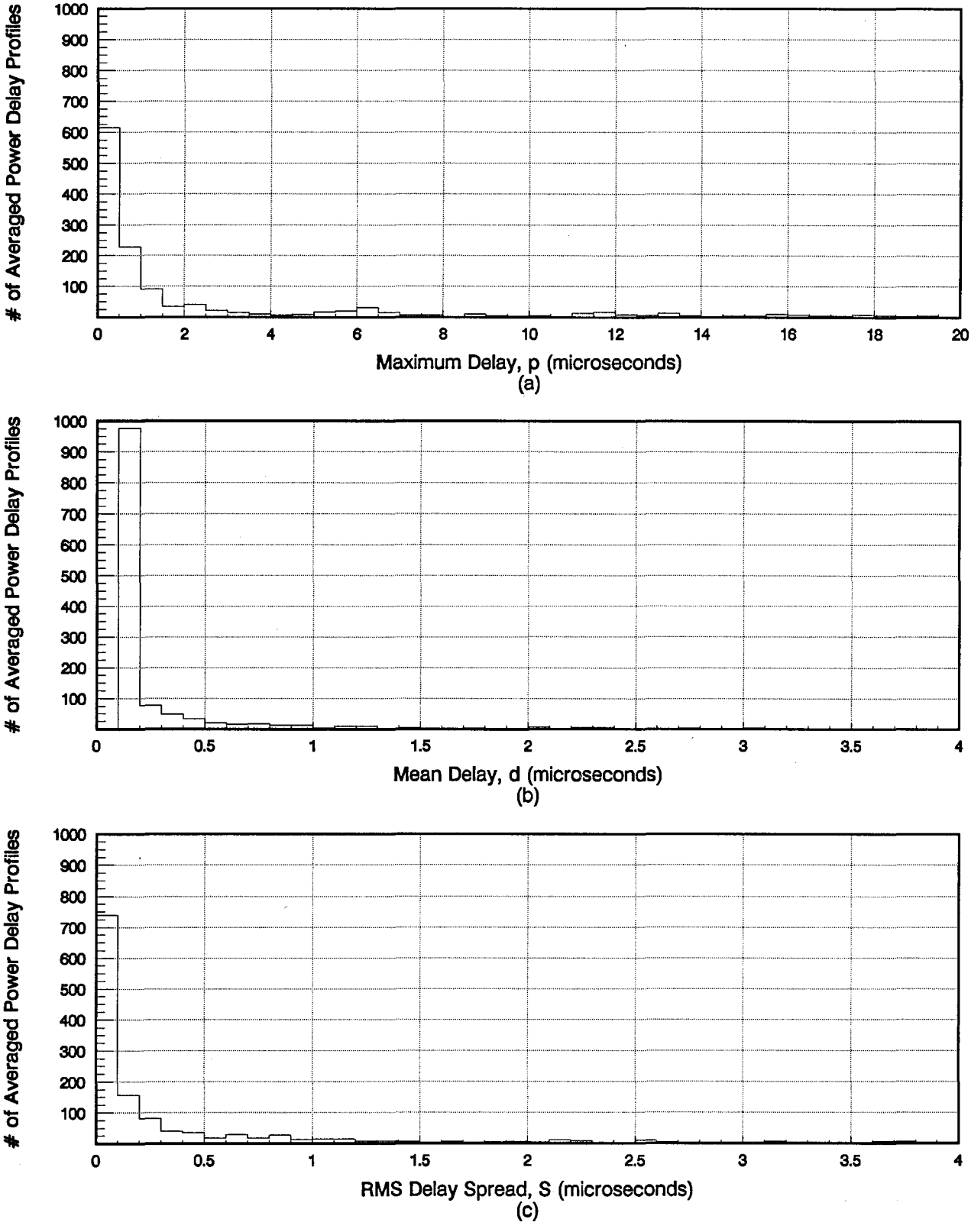

Figure 5.2. Histograms of maximum delay (a), mean delay (b), and RMS delay spread (c) for the hilly rural cell using a threshold 20 dB below the peak in each APDP.

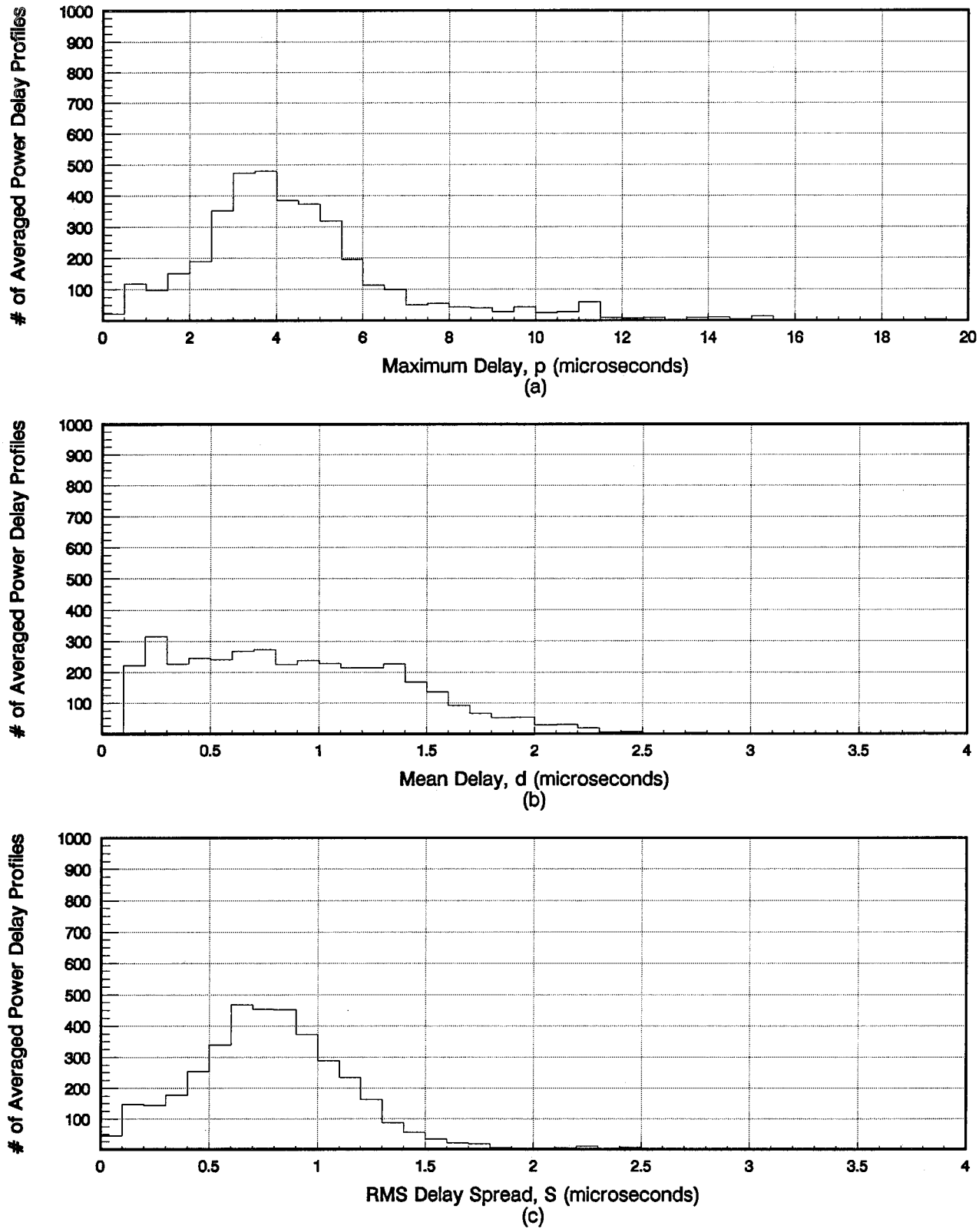

Figure 5.3. Histograms of maximum delay (a), mean delay (b), and RMS delay spread (c) for the urban high-rise cell using a threshold 20 dB below the peak in each APDP.

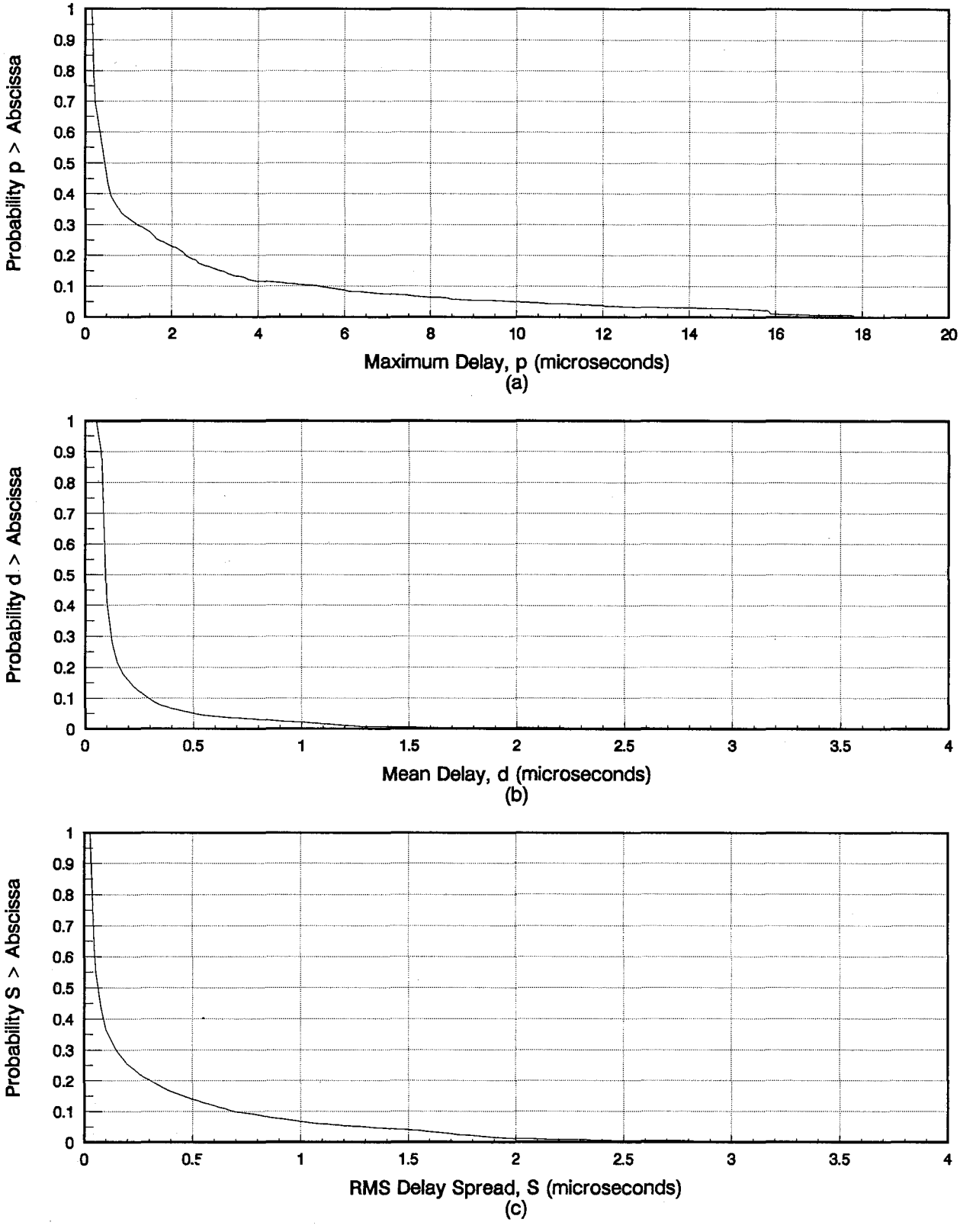

Figure 5.4. Cumulative distributions of maximum delay (a), mean delay (b), and RMS delay spread (c) for the flat rural cell using a threshold 20 dB below the peak in each APDP.

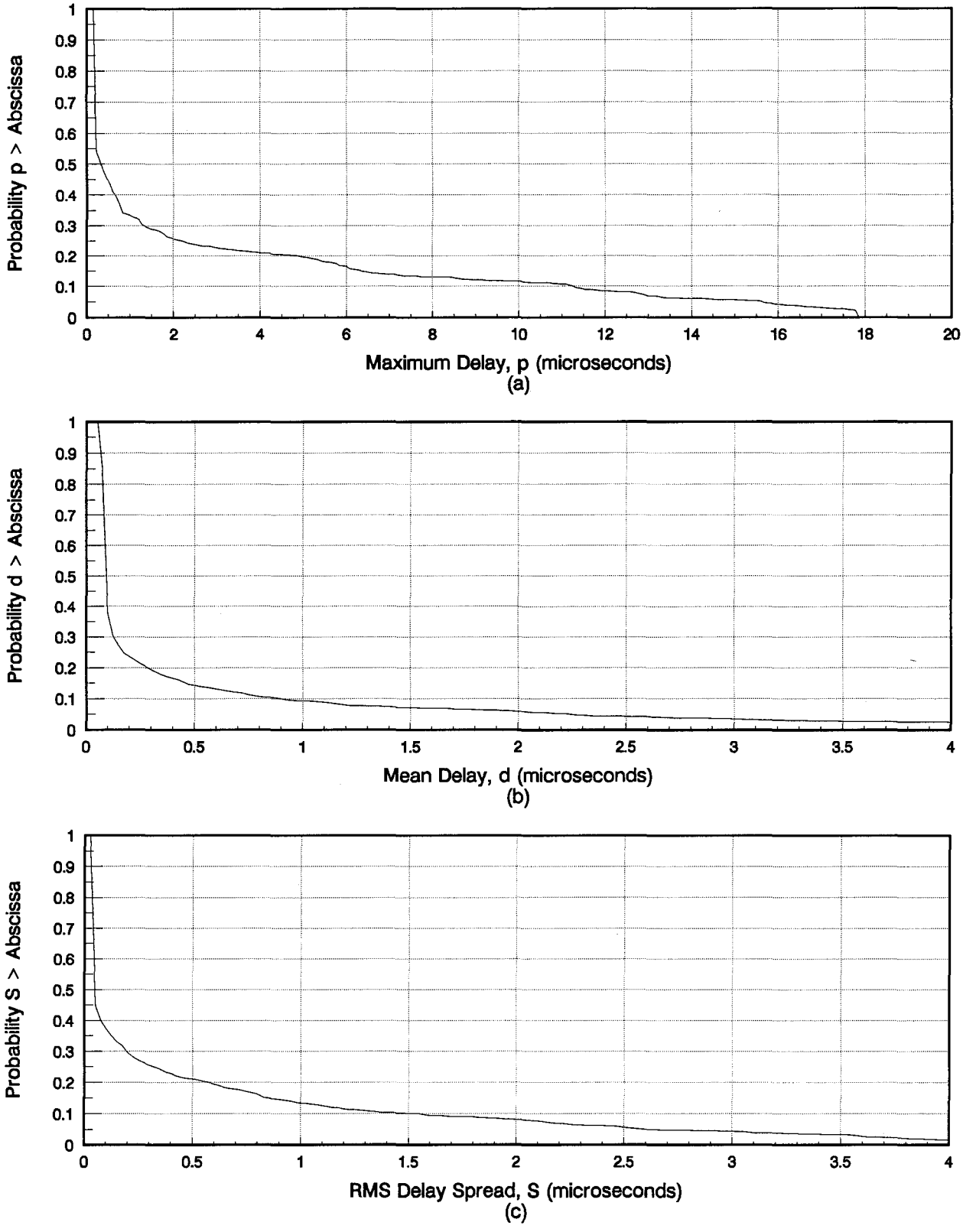

Figure 5.5. Cumulative distributions of maximum delay (a), mean delay (b), and RMS delay spread (c) for the hilly rural cell using a threshold 20 dB below the peak in each APDP.

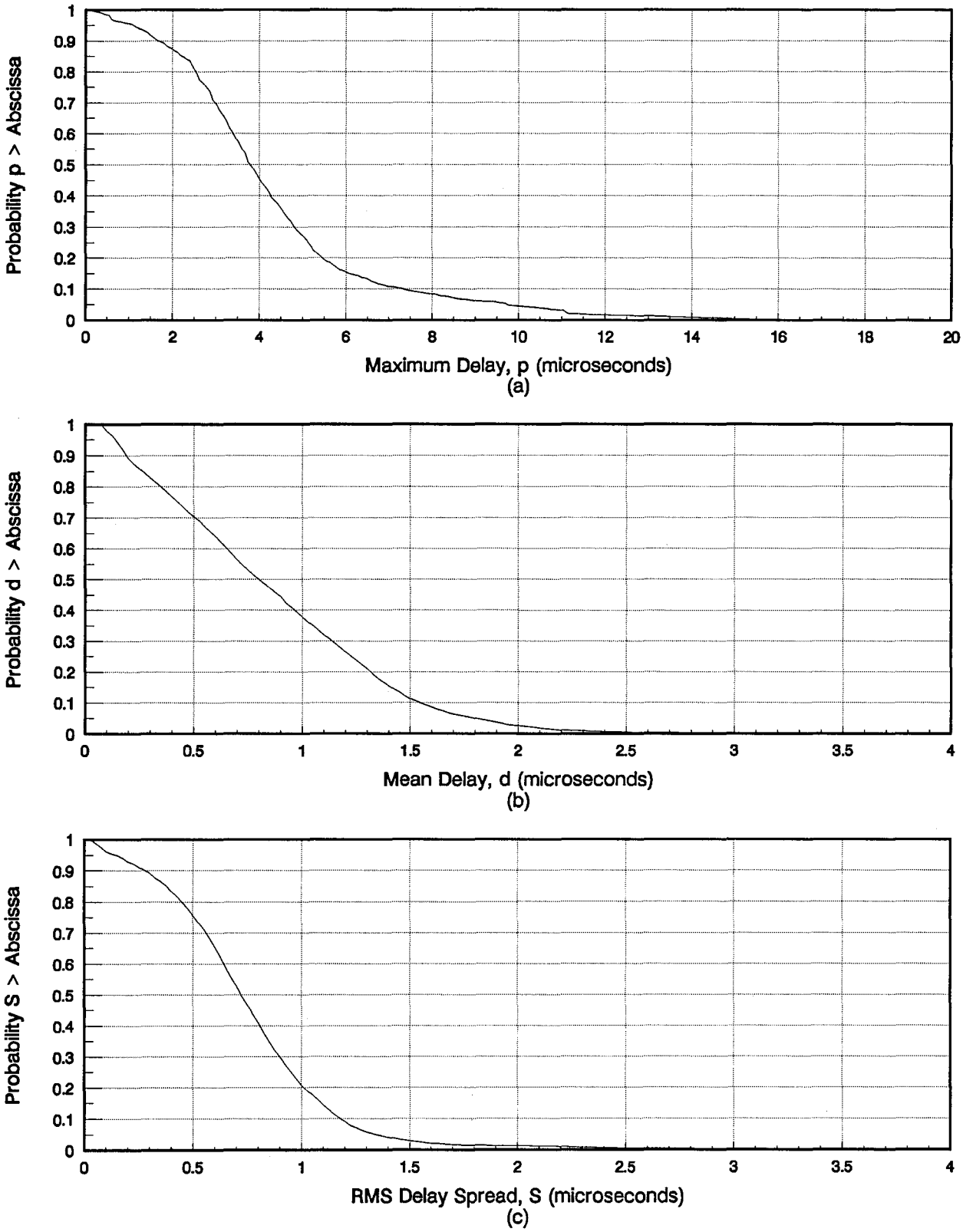

Figure 5.6. Cumulative distributions of maximum delay (a), mean delay (b), and RMS delay spread (c) for the urban high-rise cell using a threshold 20 dB below the peak in each APDP.

In the hilly rural cell, the cumulative distributions of maximum delay, mean delay, and RMS delay spread show higher probabilities of exceeding large delay values than in the other cells. The cumulative distribution of maximum delay shows a higher probability of exceeding delays 6 μs or more than in the other cells. This tends to indicate that there were more signals with delays greater than 6 μs received in the hilly rural cell compared to the other cells. This may have been due to reflections off of the foothills of the Rocky Mountains nearby.

5.2 Effects of Spatial Diversity

The measurements were taken to allow the effects of spatial diversity to be analyzed. Spatial diversity was accomplished by transmitting one BPSK PN code sequence and receiving this code on two identical receive channels. These two receive channels had antennas that were spaced 15 wavelengths apart. The effects of spatial diversity can be determined in many ways. Only one of these methods is presented here. The method presented is based on RMS delay spread values of the APDPs from both channels. This method compares the cumulative distributions of RMS delay spread for Channel 1, for Channel 2, and for the lowest RMS delay spread between both channels (hereafter called the diversity combination). The lowest RMS delay spread is found by first taking the RMS delay spread of each pair of APDPs computed from simultaneously taken PDPs on both channels (one on Channel 1 and one on Channel 2). The RMS delay spread that is the lowest between the two channels is then chosen. This process is repeated for all pairs of APDPs for each cell and the cumulative distribution for each cell is then formed.

Figure 5.7 shows the cumulative distributions of RMS delay spread for the flat rural, hilly rural, and urban high-rise cells. For each cell, the cumulative distributions of RMS delay spread are shown for Channel 1, Channel 2, and the diversity combination of the two channels. Within each cell, observe that the cumulative distributions for Channel 1 and Channel 2, separately, are nearly identical. This result is to be expected since the cumulative distribution for Channel 1 or Channel 2 is a statistical description of the RMS delay spread behavior in an entire cell over a large number of samples. Therefore, regardless of how the RMS delay spread values compare between a given APDP on Channel 1 and the corresponding APDP formed from PDPs taken simultaneously on Channel 2, the cumulative distributions for each channel separately within a given cell should be quite similar. The cumulative distribution for the diversity combination shows a lower probability of exceeding an RMS delay spread value in all three cells than for Channel 1 or Channel 2 separately. This result is most pronounced in the urban high-rise cell. Some improvement is obtained (where improvement is measured as a lower cumulative distribution of RMS delay spread) by using spatial diversity and the diversity combination technique of selecting the lowest RMS delay spread from both channels for every received impulse response. These results suggest that the wideband signals seen on each channel are indeed uncorrelated to some degree. If these signals were correlated, one would expect to see no difference in the cumulative distributions of RMS delay spread between Channel 1, Channel 2, and the diversity combination of the two channels.

5.3 Multipath Power Statistics

The multipath power statistics provide statistical information about the signal amplitude for every delay time for all of the APDPs in a given cell. These statistics include, as a function of delay time: average multipath power, standard deviation of multipath power, peak multipath power,

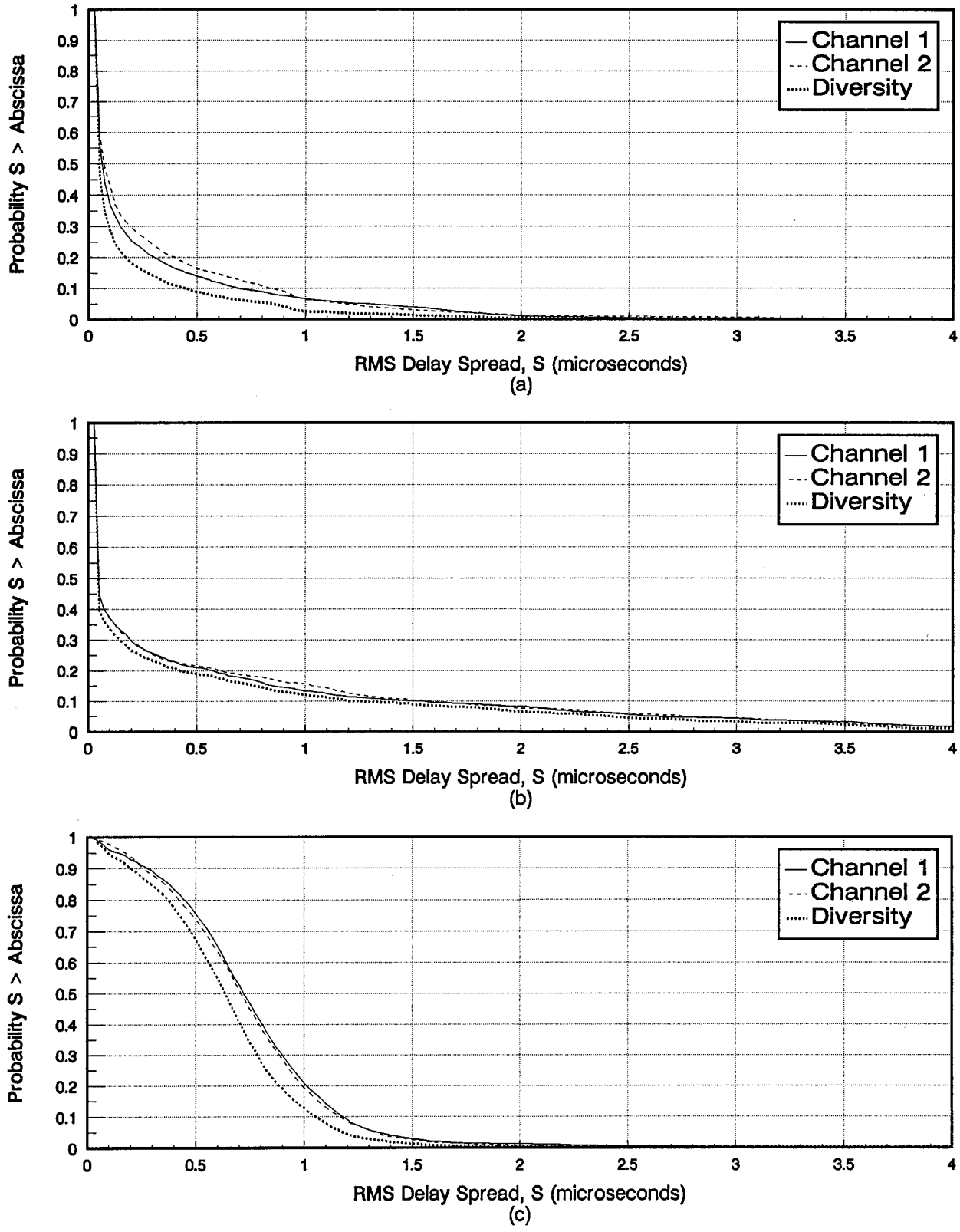

Figure 5.7. Effects of spatial diversity in the flat rural (a), hilly rural (b), and urban high-rise (c) cells.

and probability of multipath power exceeding a threshold. Each of these types of statistics will be described in this section.

All of the multipath power statistics, like the delay statistics, are computed from the APDPs. For computation of the delay statistics, the delay values are computed for each APDP separately, then the statistics are developed. The amplitude relationship between the APDPs is not important for the computation of the delay statistics. For computation of multipath power statistics, however, the amplitude relationship between APDPs is important. Therefore, some type of amplitude normalization of the APDPs is required. Each APDP is normalized by shifting the entire APDP in power such that the peak sample in the APDP is set to 0 dB. This allows APDPs of varying total power to be treated on an equivalent basis.

The average multipath power shows the average power of a delayed signal at a given delay time for the data in each cell. Average multipath power as a function of delay time is computed as

$$P_{avg}(\tau_k) = \frac{1}{M} \sum_{i=1}^{M} P_i(\tau_k)$$

where M is the total number of normalized APDPs for a given cell, τ_k is the time delay of the k^{th} sample in the APDP relative to the time of occurrence of the first perceptible reception of the transmitted signal (i.e., relative to time zero), and $P_i(\tau_k)$ is the value of the i^{th} APDP at a time delay of τ_k. The peak value in the plots of average multipath power *vs* delay time will usually be less than 0 dB. This is because the APDPs are aligned in time according to the first perceptible reception of the transmitted signal, not according to the peak sample in the APDP.

The standard deviation of multipath power shows the standard deviation of a delayed signal's power at a given delay time for the data in each cell. The standard deviation of multipath power as a function of delay time is given as

$$P_{std}(\tau_k) = \left[\frac{1}{M} \sum_{i=1}^{M} P_i^2(\tau_k) - P_{avg}^2(\tau_k) \right]^{\frac{1}{2}}.$$

The peak multipath power shows the largest signal power that was observed at a given delay time for the data in each cell. Peak multipath power is computed by finding the largest signal power at each delay time in all of the normalized APDPs for the data in each cell.

Since each individual APDP is normalized so that the peak received multipath signal is set to 0 dB, and since the first perceptible received copy of the signal is aligned to zero time, many of the values on the peak multipath plots up to 3 μs are 0 dB. This happens because the peak received multipath signal frequently occurs some time after the first perceptible received signal. This occurs when a received copy of the signal with the greatest power follows a route between the transmitter and receiver that is longer than the first received signal (as is often the case during non-line-of-sight transmitter/receiver orientation). In the graphs of average multipath power *vs* delay, the power normalization and time alignment result in having all points on the graph lie somewhere below 0 dB.

The last type of multipath power statistic is the probability of multipath power exceeding a threshold. For the data in each cell, these statistics are computed by finding the probability that a delayed signal's power will be greater than a given threshold for each delay time. The computation is performed for each delay time by finding the number of normalized APDPs for the data in a given cell in which the delayed signal power exceeds the threshold. This number

is then divided by the total number of normalized APDPs in that cell. Four different threshold levels are used: -5, -10, -15, and -20 dB, where 0 dB represents the power of the peak sample in each normalized APDP.

The average multipath power and the associated standard deviation *vs* delay time are shown in Figures 5.8a-5.10a for the flat rural, hilly rural, and urban high-rise cells, respectively. The average multipath power curves for the two rural cells are similar, with both having a narrow peak close to 0 dB that rapidly decreases to -20 dB at about 0.5 μs of delay. The average multipath power is much higher for every delay time out to about 3 μs in the urban high-rise cell as compared to the rural cells. The standard deviation curves tend to follow the average power curves until the average power curves drop down to -20 dB.

Figures 5.8b-5.10b show the peak multipath power *vs* delay time for the flat rural, hilly rural, and urban high-rise cells, respectively. Note that in all cells there is a general tendency as the delays get longer in time for the peak amplitudes to decrease. The hilly rural cell shows the highest and the urban high-rise cell shows the lowest peak amplitudes for delay times greater than 15 μs. The urban high-rise cell has the highest peak amplitudes for delay times up to about 3 μs. The standard deviation curves (Figures 5.8a-5.10a) have peaks that correspond to large amplitudes in the peak multipath power curves.

The threshold statistics *vs* delay time are displayed in Figures 5.8c-5.10c for the flat rural, hilly rural, and urban high-rise cells, respectively. For each graph, the top curve represents the probability of the normalized multipath power exceeding -20 dB. The second, third, and fourth curves from the top represent the probability of the normalized multipath power exceeding -15, -10, and -5 dB, respectively. The urban high-rise cell shows a much higher percentage of APDPs that are above threshold than the rural cells. For example, in the urban high-rise cell, 64% of the APDPs have delayed signals above the -20 dB threshold at a delay time of 1 μs. In the flat rural cell, only 5% of the APDPs have delayed signals above the -20 dB threshold at a delay time of 1 μs. As the threshold level is increased, the percentage of APDPs above threshold decreases. As an example of this, consider the urban high-rise cell. At a delay time of 2 μs, 41%, 18%, 7%, and 1% of the APDPs have signals above the -20, -15, -10, and -5 dB thresholds, respectively.

The multipath power statistics show again that the urban high-rise cell has by far more multipath components above threshold than the rural cells (out to 4 or 5 μs in delay). These statistics also show that the peak (normalized) multipath power for very long delays (greater than 15 μs) is the highest in the hilly rural cell and the lowest in the urban high-rise cell.

5.4 Number of Paths, Path Arrival Time, and Path Power Statistics

The goal of the presentation of the statistics in this section is to provide information to assist in the development of impulse response models (primarily tapped delay models) of the radio channel. The first type of statistic presented is a cumulative distribution of the number of paths that exceed a threshold. This statistic is generated for each cell by first determining the number of paths that exceed a threshold (within a 100-ns resolution) in a single APDP. This process is repeated for all of the APDPs within each cell and cumulative distributions showing the probability of meeting or exceeding a number of paths are developed for each cell. Four different threshold levels are used: -20, -10, -5, and -3 dB (where the peak sample in each APDP is 0 dB). For the -20 dB threshold, a path is identified in one of two ways. First, if four consecutive samples in the APDP (spaced 25 ns apart) are all above the -20 dB threshold and

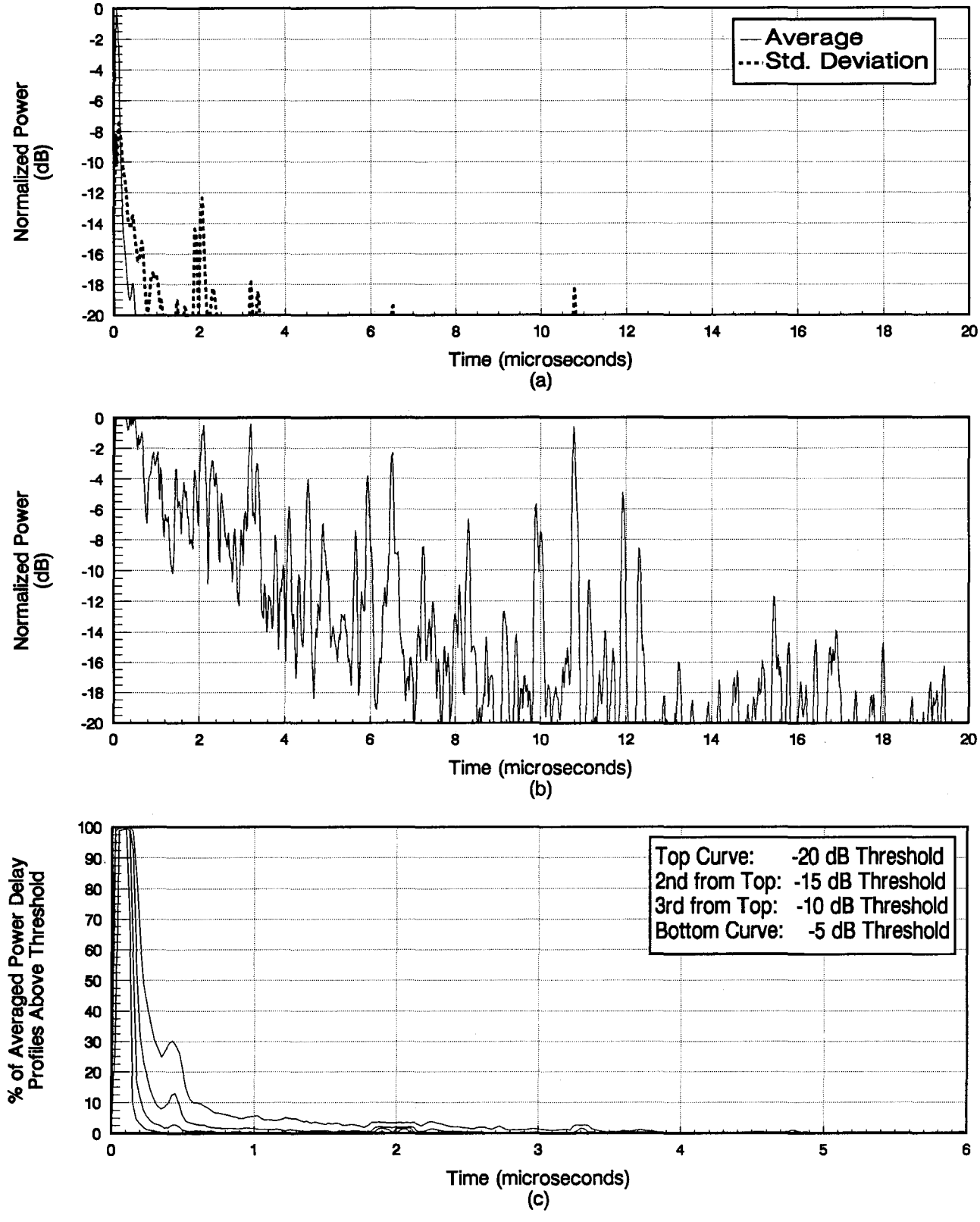

Figure 5.8. Average and standard deviation of power (a), peak power (b), and threshold statistics (c) for the flat rural cell.

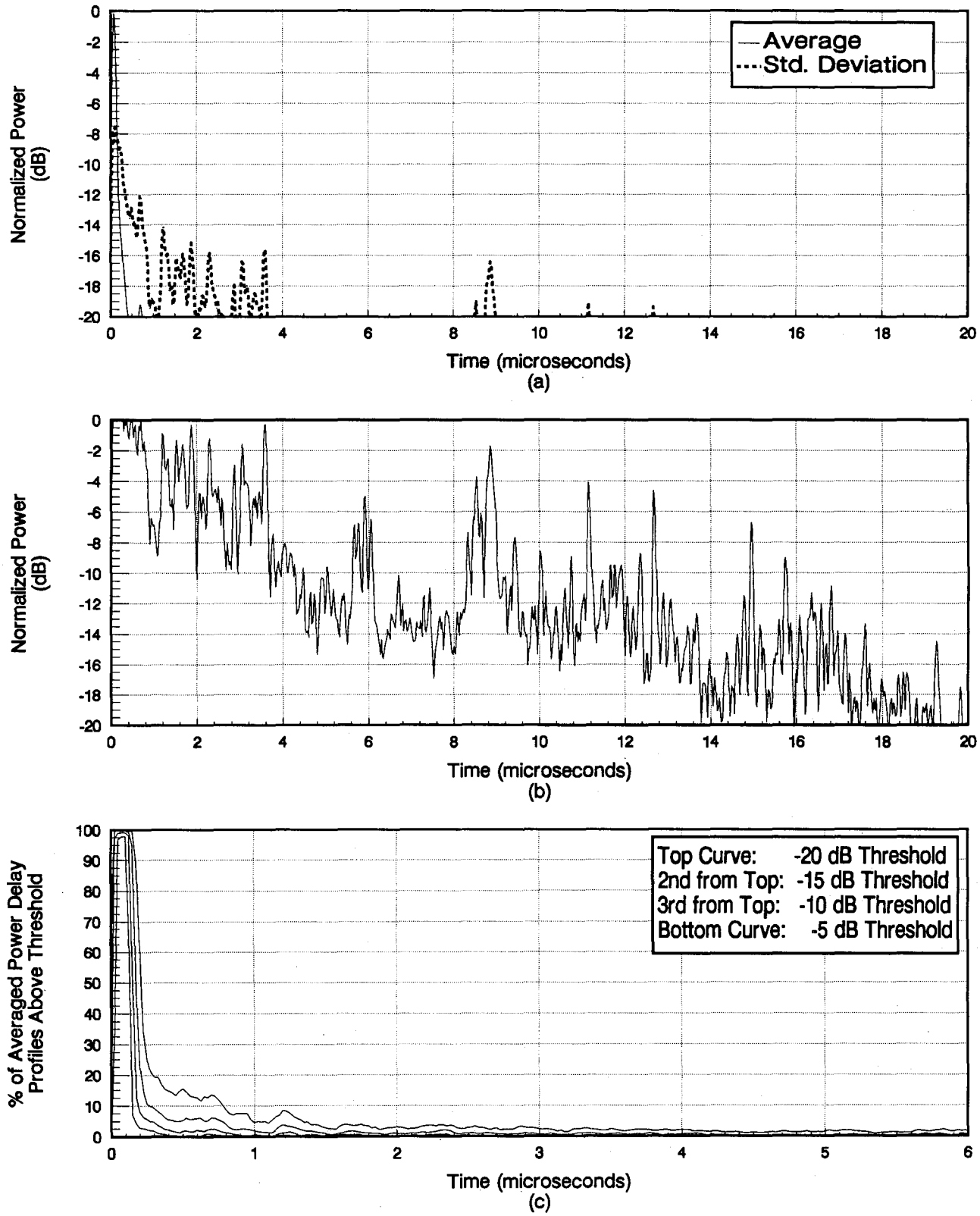

Figure 5.9. Average and standard deviation of power (a), peak power (b), and threshold statistics (c) for the hilly rural cell.

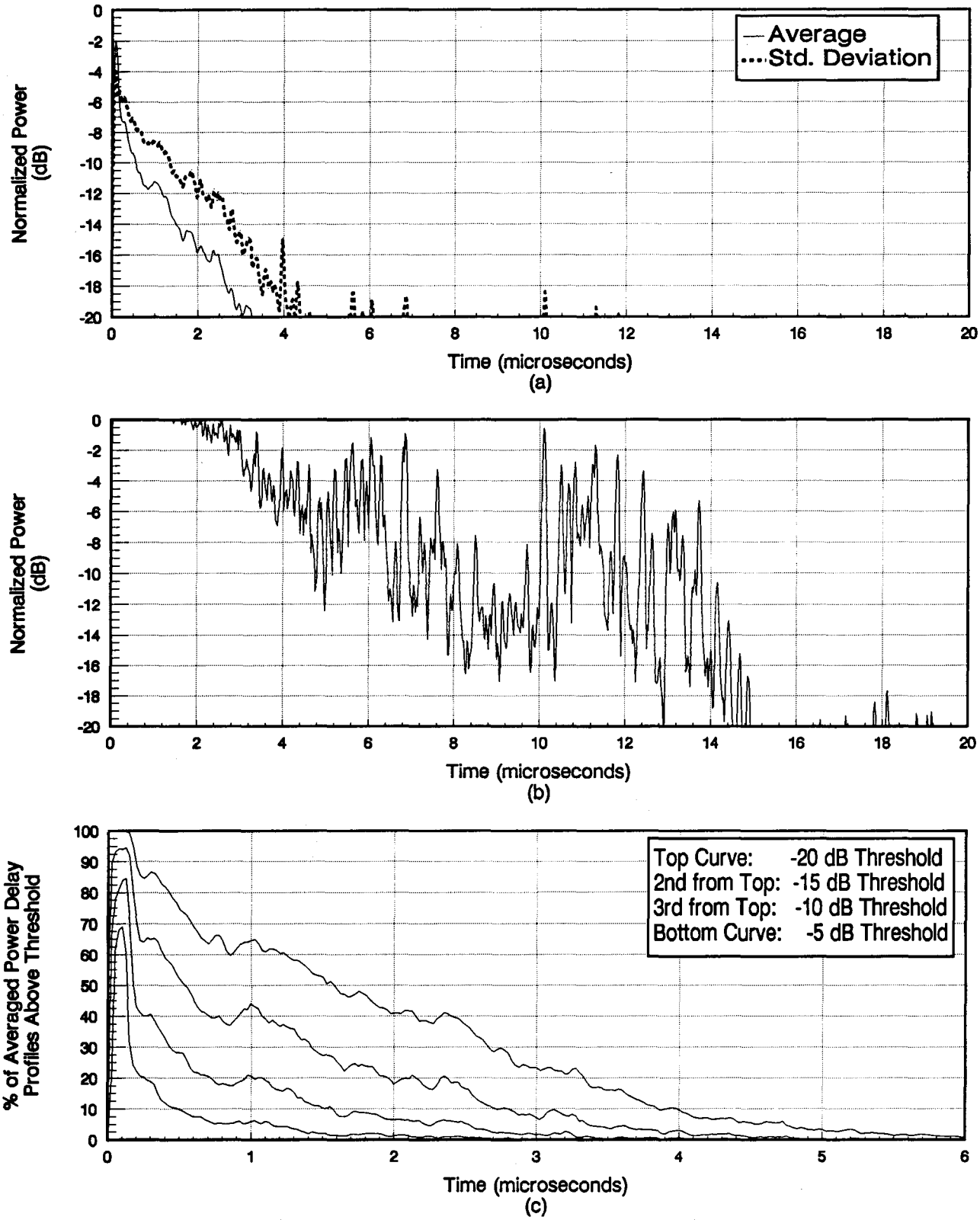

Figure 5.10. Average and standard deviation of power (a), peak power (b), and threshold statistics (c) for the urban high-rise cell.

are continually increasing in power, a path is identified. Second, if a sample in the APDP is of higher power than the next sample, a path is identified. Once a path is identified, three samples (spaced 25 ns apart) are skipped and the search for a new path begins on the next sample (i.e., on the fourth sample from the sample where the last path was identified). Skipping three samples before beginning to look for a new path ensures that no more than one path is identified within the resolution of the measurement system (100 ns). Identification of paths for the other threshold levels begins with the paths that were identified for the -20 dB threshold. Each of these paths is tested to see if it can still be counted as a path for the new threshold level.

The cumulative distributions of the number of paths are shown in Figure 5.11 for the flat rural (a), hilly rural (b), and urban high-rise (c) cells. All four thresholds are shown on each graph. The top curve represents the cumulative distribution using the -20 dB threshold, the second and third curves from the top represent the cumulative distributions for the -10 and -5 dB thresholds, respectively, and the bottom curve represents the cumulative distribution for the -3 dB threshold. Note that in the rural cells, the curves for the -5 and -3 dB thresholds are nearly identical. The probability of having APDPs with 2 or more paths is less than 0.09 in both of these cells for these threshold levels. Both of the rural cells show a somewhat higher probability of having APDPs with 2 or more paths when using the -10 dB threshold. There is a probability of about 0.26 and 0.20 of having APDPs with 2 or more paths in the flat rural and hilly rural cells, respectively. The curves for the -20 dB threshold show a much greater probability of meeting or exceeding a given number of paths than for the other threshold levels in all of the cells. In the flat rural cell, about 10% of the APDPs have 8 or more paths. About 10% of the APDPs have 13 or more paths in the hilly rural cell while about 10% of the APDPs have 33 or more paths in the urban high-rise cell. The urban high-rise cell shows a greater probability of meeting or exceeding a given number of paths than the rural cells for all threshold levels.

These results give an idea of the number of required taps that may be needed to model the impulse response of the radio channel (within a 100-ns resolution) in different environments in the 1850-1990 MHz band. The urban high-rise cell would, of course, require the largest number of taps. Note that the number of paths is quite dependent on the chosen threshold level; as the threshold level is set increasingly further below the peak of the APDPs, the number of paths increases.

The second set of statistics computed here are the path arrival time and path power statistics. These statistics give a description of the time-of-arrival and power of each path that exceeds a threshold for all APDPs within a cell that have n paths (where n varies from 1 to 10). The results are displayed in a table where the mean and standard deviation of the arrival time and power for each individual path are presented. Arrival time is relative to the time-of-occurrence of the first path in each APDP. The mean and standard deviation of power are shown in dB with respect to the peak value in the normalized APDPs. Recall that the peak value in the normalized APDPs is set to 0 dB. Tables 5.1-5.3 show the time-of-arrival and path power statistics using a -20 dB threshold for the flat rural, hilly rural, and urban high-rise cells, respectively. Tables 5.4-5.6 show the corresponding tables using the -10 dB threshold. These tables are organized so that each column represents all of the APDPs within a cell that have n paths where n varies from 1 to 10. Each row represents a specific individual path for APDPs having a total of n paths.

For an example of the use of these tables, consider Table 5.1. Choose the column with 3 paths (n=3). The number of APDPs having 3 paths was 765 out of a total number of 3220 APDPs taken in this cell. The first path always occurs at zero time therefore its mean and standard deviation of arrival time are both zero. The mean power is -0.1 dB with a standard deviation

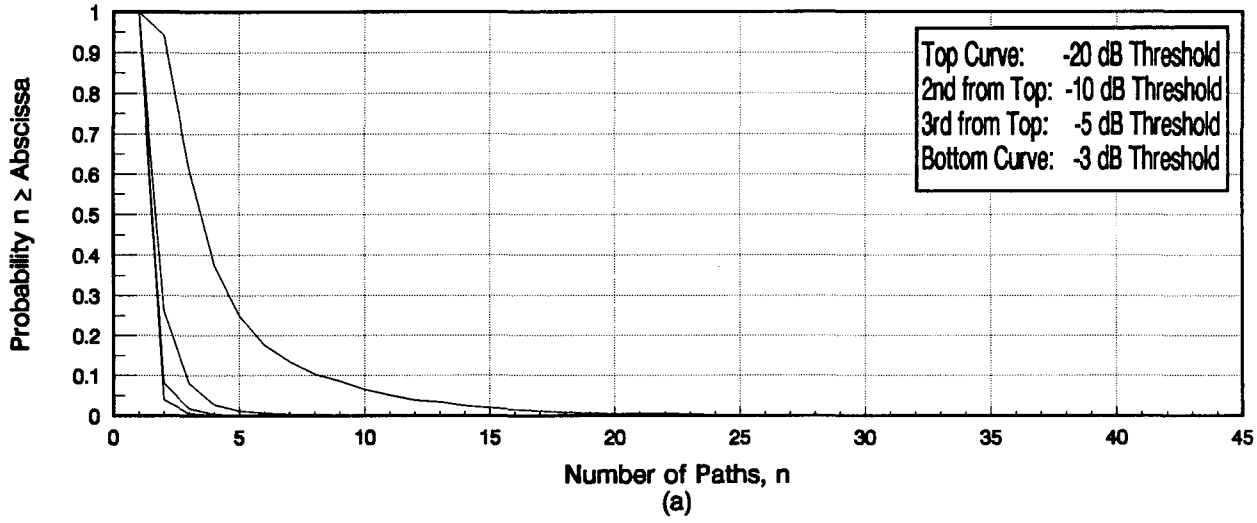

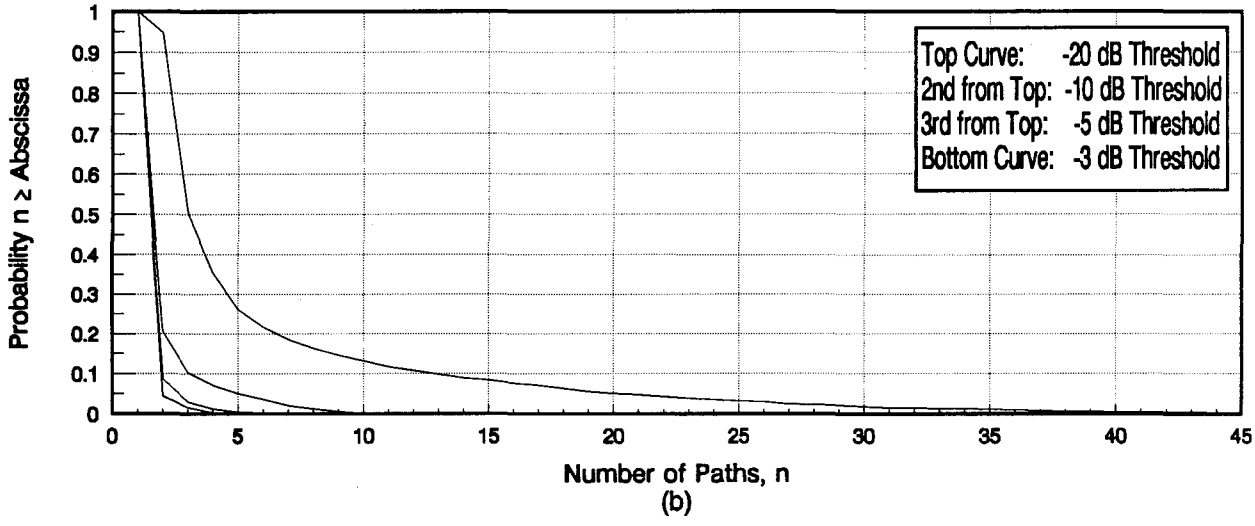

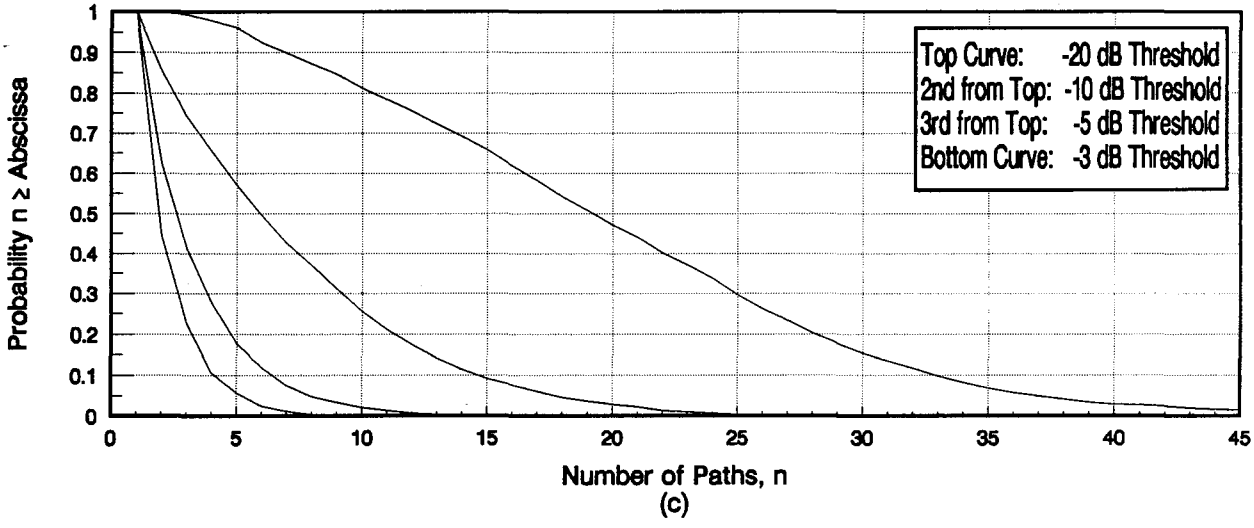

Figure 5.11. Cumulative distributions of the number of significant paths for different thresholds for the flat rural (a), hilly rural (b), and urban high-rise (c) cells.

Table 5.1. Mean (μ) and Standard Deviation (σ) of Path Arrival Time (in μs) and Path Power (in dB) Using a -20 dB Threshold for Each Individual Path for APDPs Having a Total of n Paths in the Flat Rural Cell

		Total Number of Paths n in APDP																			
		n = 1		n = 2		n = 3		n = 4		n = 5		n = 6		n = 7		n = 8		n = 9		n = 10	
Number of APDPs Having n Paths*		183		1058		765		410		236		130		102		60		64		45	
Path #		μ	σ	μ	σ	μ	σ	μ	σ	μ	σ	μ	σ	μ	σ	μ	σ	μ	σ	μ	σ
1	Time	0.00	0.00	0.00	0.00	0.00	0.00	0.00	0.00	0.00	0.00	0.00	0.00	0.00	0.00	0.00	0.00	0.00	0.00	0.00	0.00
	Power	0.0	-	0.0	-15.5	-0.1	-12.3	-0.1	-11.0	-0.1	-11.0	-0.2	-8.4	-0.3	-8.2	-0.3	-7.7	-0.4	-7.0	-0.6	-6.1
2	Time			0.17	0.43	0.14	0.21	0.15	0.75	0.11	0.03	0.19	0.83	0.11	0.04	0.27	1.21	0.11	0.03	0.12	0.03
	Power			-13.7	-14.6	-12.2	-10.6	-10.8	-9.7	-9.6	-8.7	-9.2	-7.7	-7.6	-7.0	-6.5	-6.3	-6.5	-6.3	-5.0	-5.2
3	Time					0.75	1.22	0.44	0.98	0.34	0.31	0.37	0.84	0.28	0.15	0.41	1.21	0.28	0.18	0.23	0.03
	Power					-14.7	-12.4	-14.4	-12.1	-12.9	-9.5	-13.1	-12.6	-11.6	-10.3	-10.5	-8.6	-11.4	-11.3	-11.3	-11.1
4	Time							1.61	2.59	0.87	0.87	0.75	0.97	0.52	0.33	0.63	1.22	0.52	0.36	0.44	0.17
	Power							-15.5	-14.2	-14.3	-11.1	-14.2	-12.5	-12.8	-11.5	-13.4	-13.2	-11.9	-11.2	-11.3	-9.3
5	Time									2.52	3.16	1.49	1.75	1.06	1.12	1.04	1.44	0.76	0.49	0.73	0.35
	Power									-15.8	-14.4	-16.1	-16.7	-14.5	-10.8	-12.8	-9.1	-13.1	-11.4	-13.7	-12.2
6	Time											3.78	3.91	1.85	1.82	1.55	1.68	1.10	0.63	1.08	0.53
	Power											-16.2	-15.9	-15.5	-15.4	-15.2	-15.3	-12.8	-8.8	-13.7	-10.7
7	Time													4.80	4.54	3.07	2.88	1.56	0.78	1.47	0.62
	Power													-16.4	-16.2	-14.3	-11.6	-13.3	-11.2	-14.2	-12.1
8	Time															6.09	4.71	2.83	2.20	1.93	0.86
	Power															-15.5	-13.2	-13.4	-9.1	-13.0	-10.9
9	Time																	5.52	4.57	2.79	1.76
	Power																	-15.7	-14.8	-15.9	-17.0
10	Time																			5.81	4.21
	Power																			-14.9	-11.9

*The total number of APDPs in the flat rural cell was 3220.

Table 5.2. Mean (μ) and Standard Deviation (σ) of Path Arrival Time (in μs) and Path Power (in dB) Using a -20 dB Threshold for Each Individual Path for APDPs Having a Total of n Paths in the Hilly Rural Cell

		Total Number of Paths n in APDP																			
		n = 1		n = 2		n = 3		n = 4		n = 5		n = 6		n = 7		n = 8		n = 9		n = 10	
Number of APDPs Having n Paths*		70		595		201		124		60		43		29		24		20		19	
Path #		μ	σ	μ	σ	μ	σ	μ	σ	μ	σ	μ	σ	μ	σ	μ	σ	μ	σ	μ	σ
1	Time	0.00	0.00	0.00	0.00	0.00	0.00	0.00	0.00	0.00	0.00	0.00	0.00	0.00	0.00	0.00	0.00	0.00	0.00	0.00	0.00
	Power	0.0	-	0.0	-13.2	-0.1	-9.9	-0.4	-5.9	-0.9	-4.6	-0.7	-5.2	-1.2	-4.2	-1.3	-3.8	-1.3	-4.3	-0.6	-5.9
2	Time			0.14	0.41	0.18	0.47	0.20	0.59	0.53	2.15	0.22	0.42	0.56	2.07	0.35	0.60	0.87	2.83	0.12	0.06
	Power			-14.6	-13.2	-12.6	-9.8	-9.1	-5.9	-7.1	-5.1	-8.6	-6.5	-6.8	-5.0	-5.9	-5.0	-5.6	-4.7	-7.1	-5.5
3	Time					1.23	2.10	0.91	1.55	0.93	2.28	0.70	1.03	1.12	2.30	1.24	2.52	1.36	2.92	0.79	1.40
	Power					-16.7	-17.1	-12.4	-8.2	-11.7	-7.9	-13.7	-11.5	-8.8	-5.9	-10.6	-7.1	-11.6	-11.2	-9.3	-8.0
4	Time							2.04	2.52	1.53	2.68	1.36	1.71	1.40	2.33	1.47	2.56	1.59	2.96	1.17	1.67
	Power							-15.7	-15.3	-11.2	-7.2	-10.9	-7.4	-11.1	-7.6	-10.0	-6.9	-14.6	-16.4	-12.0	-12.2
5	Time									3.28	4.26	2.04	2.05	2.20	2.74	1.95	2.64	2.11	3.07	1.46	1.67
	Power									-14.0	-10.5	-10.4	-6.7	-10.0	-7.0	-12.2	-10.5	-10.8	-6.7	-11.5	-8.2
6	Time											4.26	4.33	4.29	4.47	3.10	3.69	2.35	3.10	2.23	2.32
	Power											-12.5	-8.1	-14.2	-12.4	-14.8	-15.7	-10.4	-6.7	-10.5	-9.0
7	Time													6.88	5.13	4.47	4.15	2.72	3.10	2.94	2.92
	Power													-15.6	-15.8	-14.4	-13.8	-13.8	-13.9	-14.0	-13.8
8	Time															7.82	4.49	4.72	4.34	3.37	3.34
	Power															-15.9	-18.1	-14.5	-13.7	-13.4	-13.2
9	Time																	7.01	4.76	4.20	3.55
	Power																	-15.7	-16.1	-15.4	-15.3
10	Time																			7.40	4.49
	Power																			-17.3	-19.4

*The total number of APDPs in the hilly rural cell was 1341.

Table 5.3. Mean (μ) and Standard Deviation (σ) of Path Arrival Time (in μs) and Path Power (in dB) Using a -20 dB Threshold for Each Individual Path for APDPs Having a Total of n Paths in the Urban High-Rise Cell

		Total Number of Paths n in APDP																			
		n = 1		n = 2		n = 3		n = 4		n = 5		n = 6		n = 7		n = 8		n = 9		n = 10	
Number of APDPs Having n Paths*		4		24		52		69		140		93		108		93		137		106	
Path #		μ	σ	μ	σ	μ	σ	μ	σ	μ	σ	μ	σ	μ	σ	μ	σ	μ	σ	μ	σ
1	Time	0.00	0.00	0.00	0.00	0.00	0.00	0.00	0.00	0.00	0.00	0.00	0.00	0.00	0.00	0.00	0.00	0.00	0.00	0.00	0.00
	Power	0.0	-	0.0	-21.7	-0.1	-12.1	-0.9	-4.3	-2.9	-3.2	-1.2	-4.0	-0.8	-4.7	-1.0	-4.4	-1.4	-4.0	-1.4	-4.0
2	Time			0.20	0.26	0.18	0.34	0.14	0.06	0.15	0.15	0.12	0.06	0.13	0.05	0.14	0.09	0.13	0.05	0.14	0.07
	Power			-13.3	-16.1	-13.3	-14.5	-7.0	-4.6	-3.0	-3.3	-5.7	-4.2	-8.0	-5.7	-6.9	-4.9	-6.1	-4.7	-6.8	-5.1
3	Time					0.81	0.99	0.55	0.55	0.33	0.27	0.29	0.12	0.30	0.13	0.31	0.13	0.28	0.10	0.29	0.17
	Power					-16.0	-17.1	-13.3	-9.1	-12.2	-9.2	-14.6	-15.8	-12.4	-8.7	-10.7	-7.4	-9.2	-6.9	-7.9	-5.5
4	Time							1.62	1.46	0.71	0.59	0.59	0.25	0.55	0.26	0.49	0.18	0.45	0.17	0.45	0.18
	Power							-15.2	-14.0	-15.9	-17.1	-14.8	-11.4	-14.2	-12.7	-12.5	-9.4	-13.1	-11.0	-10.5	-7.7
5	Time									1.54	1.36	1.08	0.57	0.92	0.48	0.78	0.31	0.71	0.25	0.69	0.24
	Power									-14.5	-15.3	-14.2	-13.1	-11.3	-7.1	-13.4	-9.7	-11.5	-7.6	-12.5	-9.9
6	Time											1.92	1.38	1.37	0.71	1.22	0.55	1.02	0.38	0.94	0.31
	Power											-16.4	-18.3	-13.5	-9.7	-13.5	-9.7	-11.2	-7.2	-12.2	-8.5
7	Time													2.50	1.94	1.75	0.91	1.40	0.53	1.28	0.46
	Power													-16.0	-15.3	-13.9	-12.5	-13.8	-11.9	-12.9	-9.7
8	Time															2.88	1.64	1.92	0.79	1.60	0.59
	Power															-15.5	-14.2	-14.1	-12.5	-12.1	-9.3
9	Time																	2.92	1.58	1.99	0.78
	Power																	-14.3	-11.9	-15.3	-15.4
10	Time																			3.03	1.83
	Power																			-16.1	-15.3

*The total number of APDPs in the urban high-rise cell was 3813.

Table 5.4. Mean (μ) and Standard Deviation (σ) of Path Arrival Time (in μs) and Path Power (in dB) Using a -10 dB Threshold for Each Individual Path for APDPs Having a Total of n Paths in the Flat Rural Cell

		Total Number of Paths n in APDP																			
		n = 1		n = 2		n = 3		n = 4		n = 5		n = 6		n = 7		n = 8		n = 9		n = 10	
Number of APDPs Having n Paths*		2371		587		172		51		18		7		4		2		3		4	
Path #		μ	σ	μ	σ	μ	σ	μ	σ	μ	σ	μ	σ	μ	σ	μ	σ	μ	σ	μ	σ
1	Time	0.00	0.00	0.00	0.00	0.00	0.00	0.00	0.00	0.00	0.00	0.00	0.00	0.00	0.00	0.00	0.00	0.00	0.00	0.00	0.00
	Power	0.0	-	-0.3	-9.0	-0.4	-6.8	-0.7	-6.1	-1.6	-4.8	-1.0	-6.0	-2.5	-4.9	-1.1	-6.5	-0.7	-8.2	-2.0	-6.7
2	Time			0.32	0.86	0.51	0.70	0.42	1.49	0.14	0.07	0.17	0.16	0.13	0.03	0.11	0.01	0.13	0.04	0.15	0.03
	Power			-6.4	-7.4	-4.9	-6.3	-4.0	-5.0	-2.4	-5.1	-3.1	-4.8	-1.9	-5.1	-5.8	-8.9	-4.2	-6.4	-3.6	-4.6
3	Time					1.38	1.97	0.98	1.69	0.34	0.17	0.36	0.15	0.41	0.19	0.38	0.15	0.28	0.05	0.23	0.03
	Power					-5.5	-7.2	-6.0	-7.4	-5.4	-6.8	-6.9	-9.8	-5.0	-8.5	-4.1	-6.0	-2.4	-4.5	-5.9	-10.2
4	Time							2.07	2.45	1.26	1.74	0.68	0.31	0.59	0.22	0.68	0.28	0.41	0.03	0.49	0.06
	Power							-5.2	-6.7	-6.8	-8.6	-8.8	-14.3	-7.2	-10.6	-2.4	-3.7	-4.6	-7.3	-5.2	-9.6
5	Time									2.93	3.86	1.25	1.01	0.83	0.13	0.85	0.30	0.51	0.06	0.68	0.10
	Power									-6.7	-7.1	-8.6	-14.9	-4.4	-7.6	-5.8	-11.9	-5.4	-7.8	-3.7	-4.8
6	Time											4.32	4.54	2.38	2.08	0.99	0.34	1.43	0.62	0.77	0.08
	Power											-5.1	-5.5	-8.9	-20.5	-6.2	-9.5	-8.7	-15.9	-5.8	-7.9
7	Time													3.24	1.86	1.23	0.43	1.53	0.59	0.90	0.07
	Power													-5.4	-7.9	-7.9	-13.1	-6.6	-13.1	-3.9	-8.7
8	Time															2.91	1.11	1.82	0.45	1.61	0.99
	Power															-7.1	-12.0	-5.2	-18.1	-4.5	-4.3
9	Time																	4.83	0.92	2.08	1.01
	Power																	-8.0	-14.0	-6.5	-13.1
10	Time																			3.12	1.94
	Power																			-3.6	-5.4

*The total number of APDPs in the flat rural cell was 3220.

Table 5.5. Mean (μ) and Standard Deviation (σ) of Path Arrival Time (in μs) and Path Power (in dB) Using a -10 dB Threshold for Each Individual Path for APDPs Having a Total of n Paths in the Hilly Rural Cell

		Total Number of Paths n in APDP																			
		n = 1		n = 2		n = 3		n = 4		n = 5		n = 6		n = 7		n = 8		n = 9		n = 10	
Number of APDPs Having n Paths*		1065		139		41		29		18		22		10		9		7		0	
Path #		μ	σ	μ	σ	μ	σ	μ	σ	μ	σ	μ	σ	μ	σ	μ	σ	μ	σ	μ	σ
1	Time	0.00	0.00	0.00	0.00	0.00	0.00	0.00	0.00	0.00	0.00	0.00	0.00	0.00	0.00	0.00	0.00	0.00	0.00	-	-
	Power	0.0	-	-0.6	-6.0	-1.1	-5.2	-0.6	-6.3	-0.9	-5.9	-1.0	-5.0	-1.3	-5.6	-1.7	-4.7	-1.1	-5.7	-	-
2	Time			0.51	1.40	0.35	0.55	1.11	1.82	0.32	0.73	0.59	0.96	0.47	0.69	0.53	1.11	0.53	0.70	-	-
	Power			-5.2	-5.5	-4.4	-5.0	-6.0	-6.9	-4.4	-5.6	-5.4	-7.0	-2.8	-5.0	-2.7	-4.7	-5.2	-8.3	-	-
3	Time					1.59	2.22	2.04	2.81	1.06	1.99	1.14	1.18	0.78	0.79	0.66	1.08	1.07	0.92	-	-
	Power					-6.5	-8.0	-5.8	-6.5	-5.4	-8.5	-6.4	-9.4	-5.2	-5.9	-4.5	-7.6	-3.5	-5.5	-	-
4	Time							3.18	3.37	1.91	3.13	1.89	1.85	1.15	0.74	0.81	1.14	1.25	0.95	-	-
	Power							-5.4	-6.5	-5.0	-5.5	-5.4	-5.7	-5.3	-7.4	-5.0	-5.3	-4.4	-5.5	-	-
5	Time									3.05	4.04	2.61	2.63	2.48	3.21	1.06	1.10	1.43	1.03	-	-
	Power									-5.5	-7.0	-5.3	-6.6	-6.4	-6.8	-3.9	-5.0	-5.4	-6.2	-	-
6	Time											5.09	4.11	4.34	4.24	1.58	1.59	1.74	1.03	-	-
	Power											-6.4	-7.2	-6.7	-8.6	-6.5	-7.8	-4.0	-5.2	-	-
7	Time													4.61	4.13	2.29	1.42	2.25	0.81	-	-
	Power													-7.8	-11.6	-6.9	-10.8	-5.8	-7.2	-	-
8	Time															2.87	1.43	2.53	0.78	-	-
	Power															-6.4	-7.5	-6.7	-9.5	-	-
9	Time																	7.39	3.48	-	-
	Power																	-7.3	-10.4	-	-
10	Time																			-	-
	Power																			-	-

*The total number of APDPs in the hilly rural cell was 1341.

Table 5.6. Mean (μ) and Standard Deviation (σ) of Path Arrival Time (in μs) and Path Power (in dB) Using a -10 dB Threshold for Each Individual Path for APDPs Having a Total of n Paths in the Urban High-Rise Cell

		Total Number of Paths n in APDP																			
		n = 1		n = 2		n = 3		n = 4		n = 5		n = 6		n = 7		n = 8		n = 9		n = 10	
Number of APDPs Having n Paths*		545		438		333		318		293		264		215		224		208		173	
Path #		μ	σ	μ	σ	μ	σ	μ	σ	μ	σ	μ	σ	μ	σ	μ	σ	μ	σ	μ	σ
1	Time	0.00	0.00	0.00	0.00	0.00	0.00	0.00	0.00	0.00	0.00	0.00	0.00	0.00	0.00	0.00	0.00	0.00	0.00	0.00	0.00
	Power	0.0	-	-1.1	-4.7	-1.5	-4.6	-1.8	-4.5	-2.1	-4.4	-2.8	-4.6	-3.2	-4.6	-3.7	-4.9	-3.3	-4.7	-3.0	-4.7
2	Time			0.66	1.12	0.31	0.36	0.29	0.29	0.23	0.23	0.22	0.23	0.21	0.21	0.20	0.17	0.20	0.16	0.20	0.18
	Power			-4.1	-4.5	-4.3	-4.9	-4.2	-5.1	-4.2	-5.0	-3.8	-4.7	-3.8	-4.8	-3.4	-4.7	-3.7	-5.0	-3.0	-4.8
3	Time					1.01	1.05	0.66	0.50	0.55	0.38	0.46	0.30	0.44	0.30	0.41	0.27	0.40	0.26	0.40	0.27
	Power					-5.3	-5.9	-4.4	-5.1	-4.9	-5.4	-4.6	-5.3	-4.4	-5.3	-4.4	-5.5	-4.3	-5.5	-4.3	-5.7
4	Time							1.45	1.17	0.95	0.53	0.75	0.42	0.69	0.38	0.65	0.35	0.62	0.30	0.58	0.28
	Power							-6.0	-6.4	-5.5	-6.3	-4.9	-5.5	-4.5	-5.3	-4.7	-5.8	-4.5	-5.7	-4.8	-5.8
5	Time									1.58	0.89	1.15	0.53	1.00	0.46	0.97	0.42	0.86	0.35	0.79	0.31
	Power									-5.9	-6.5	-6.0	-6.8	-5.4	-6.0	-4.6	-5.3	-5.1	-5.8	-4.4	-5.4
6	Time											1.75	1.02	1.33	0.53	1.29	0.52	1.12	0.41	1.02	0.35
	Power											-5.9	-6.4	-6.3	-7.2	-5.9	-6.7	-5.0	-5.8	-5.8	-6.5
7	Time													1.92	0.91	1.68	0.65	1.41	0.51	1.29	0.43
	Power													-6.6	-7.2	-6.2	-6.8	-5.4	-6.2	-5.0	-6.0
8	Time															2.15	0.88	1.74	0.61	1.55	0.49
	Power															-5.9	-6.5	-6.2	-7.2	-6.0	-7.2
9	Time																	2.30	1.04	1.86	0.60
	Power																	-6.4	-7.4	-6.3	-7.6
10	Time																			2.30	0.89
	Power																			-6.7	-7.9

*The total number of APDPs in the urban high-rise cell was 3813.

of -12.3 dB. The mean arrival time of the second path is 0.14 μs with a standard deviation of 0.21 μs. The corresponding mean power is -12.2 dB with a standard deviation of -10.6 dB. Values for these parameters are found in a similar manner for the third path.

The cumulative distributions of the number of paths give an indication of how helpful the time-of-arrival and path power information will be in the design of impulse response models. For the -20 dB threshold, about 95%, 89%, and 22% of the APDPs had a maximum of 10 paths in the flat rural, hilly rural, and urban high-rise cells, respectively. This shows that using a -20 dB threshold, 10 paths can adequately represent most of the APDPs in the rural cells but not in the urban high-rise cell. Hence, the time-of-arrival and path power information using the -20 dB threshold should be quite helpful in the design of impulse response models for cells similar to the rural cells in this study. For the -10 dB threshold, almost 100% of the APDPs in the rural cells and about 79% of the APDPs in the urban high-rise cell had a maximum of 10 paths. This shows that using a -10 dB threshold, 10 paths can adequately represent most of the APDPs in all of the cells. The information shown in Tables 5.4-5.6 should therefore be quite helpful in the design of impulse response models for cells similar to those used in this study.

5.5 Correlation Bandwidth

The correlation bandwidth (sometimes called coherence bandwidth) is the bandwidth in which the spectral components of the transmitted signal are affected in a similar way [6]. In order to find the correlation bandwidth, the autocorrelation of the frequency transfer function of the channel must be determined. An easy way to obtain this autocorrelation is by taking the Fourier transform of $|h(t)|^2$, the magnitude squared of the complex impulse response of the channel [7]. Since the APDPs are digitized, bandlimited approximations to $|h(t)|^2$, they may be used to obtain approximations to the autocorrelation of the frequency transfer function.

The procedure to compute correlation bandwidth therefore begins by taking the discrete Fourier transform of each APDP. The magnitude of this quantity is given as $|G(jf_k)|$ and represents an approximation to the magnitude of the autocorrelation of the frequency transfer function of the channel. Note that f_k is the frequency of the k^{th} point along the spectrum and ranges from 0 to 20 MHz. The discrete Fourier transform is then taken of a PDP generated from the measurement system with the transmitter and receiver connected via a coaxial cable and attenuator as in the amplitude calibration setup. The magnitude of this quantity is given as $|F(jf_k)|$. The effects of the measurement system are removed by dividing $|G(jf_k)|$ by $|F(jf_k)|$ [4]. The resulting magnitude spectrum is then used to determine the 90%, 77%, 63%, and 50% correlation bandwidths ($Bc_{0.9}$, $Bc_{0.77}$, $Bc_{0.63}$, and $Bc_{0.5}$) by finding the frequencies at which the magnitude is 90%, 77%, 63%, and 50% of the peak value, respectively. For the data in each cell, histograms of $Bc_{0.9}$ and $Bc_{0.5}$ are then computed. Cumulative distributions of $Bc_{0.9}$, $Bc_{0.77}$, $Bc_{0.63}$, and $Bc_{0.5}$ are also computed.

The histograms for both the 50% and 90% correlation bandwidths show the number of APDPs having correlation bandwidth values that fall within 0.5-MHz bins. Figures 5.12a-5.14a show the histograms for $Bc_{0.5}$ for the flat rural cell, hilly rural cell, and urban high-rise cell, respectively. Both of the rural cells show a similar distribution of $Bc_{0.5}$. The distributions in these cells are quite spread out, with $Bc_{0.5}$ values occurring most frequently in the 15 to 16 MHz range. The distribution in the urban high-rise cell is dramatically different. This distribution is substantially narrower, with $Bc_{0.5}$ values occurring most frequently between 0.5 and 1 MHz.

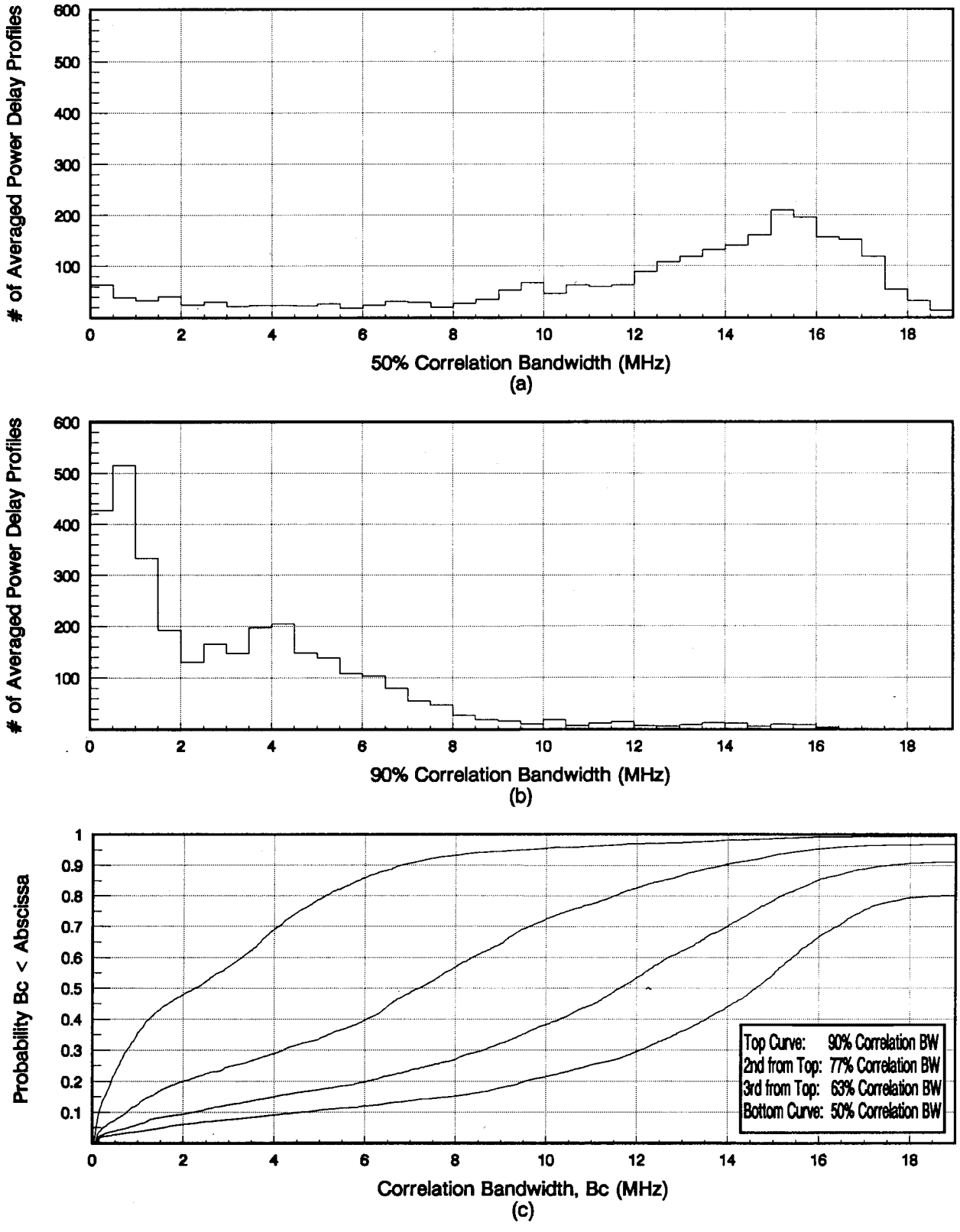

Figure 5.12. Histograms (a-b) and cumulative distributions (c) of correlation bandwidth for the flat rural cell.

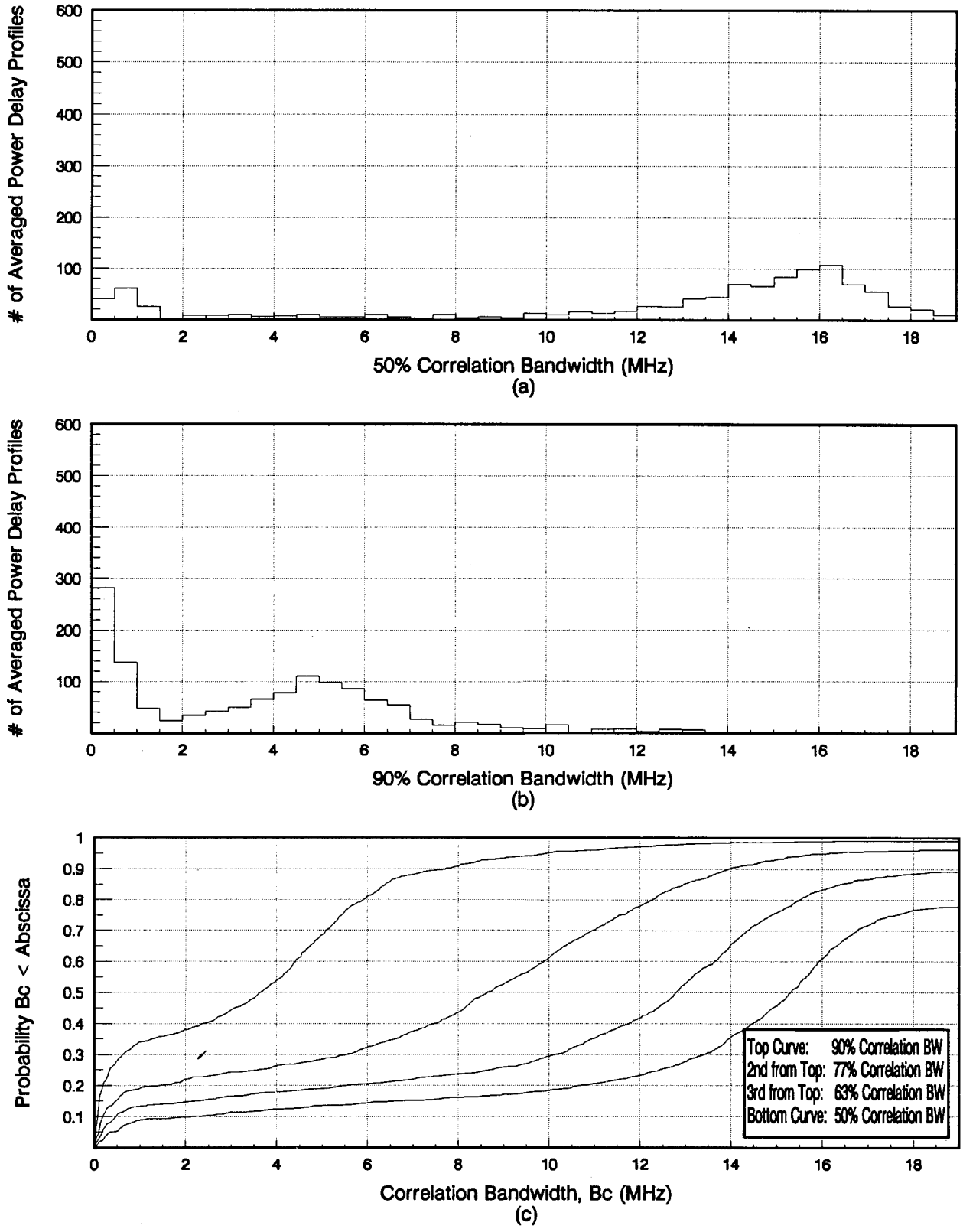

Figure 5.13. Histograms (a-b) and cumulative distributions (c) of correlation bandwidth for the hilly rural cell.

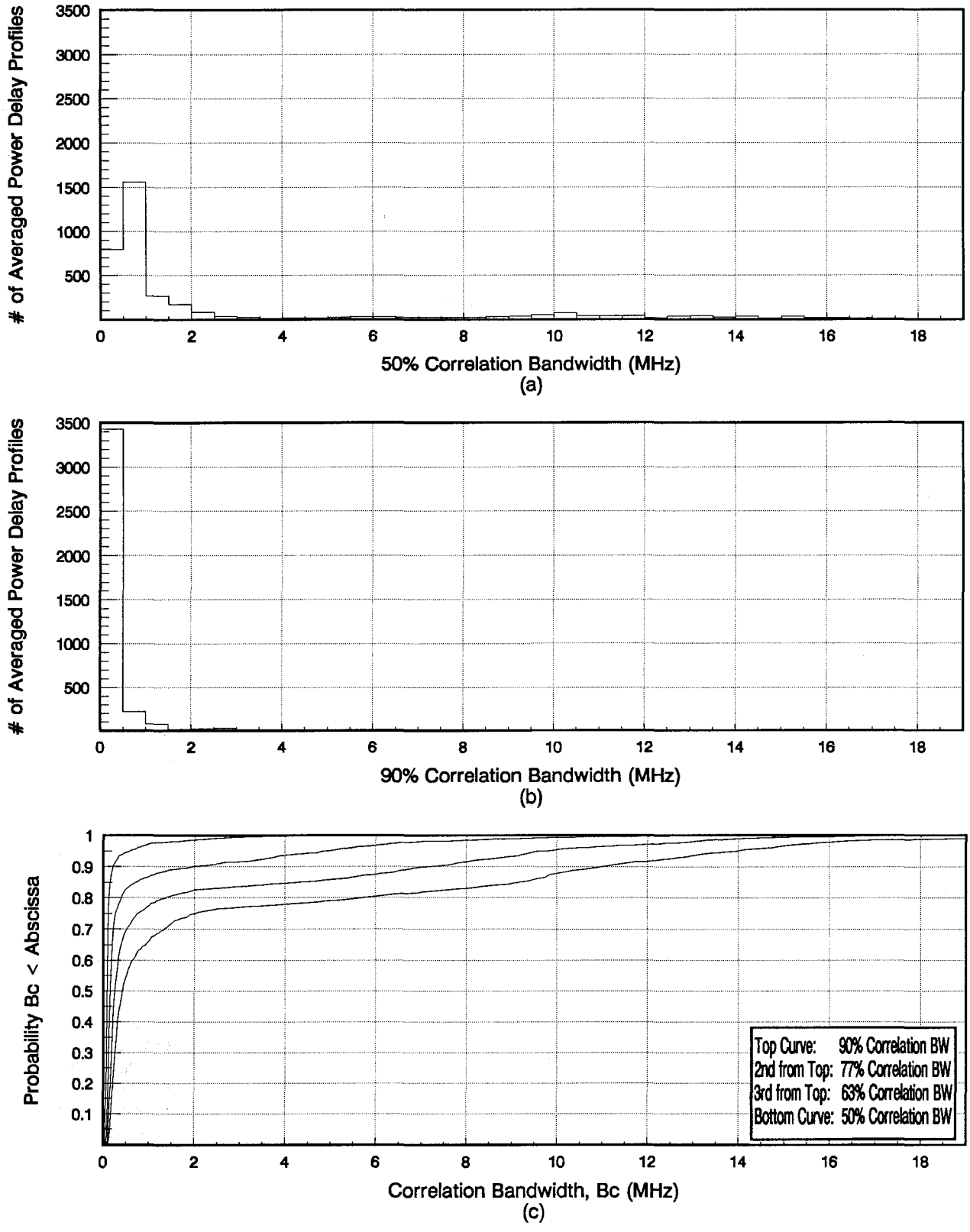

Figure 5.14. Histograms (a-b) and cumulative distributions (c) of correlation bandwidth for the urban high-rise cell.

Figures 5.12b-5.14b show the histograms for $Bc_{0.9}$ for the flat rural cell, hilly rural cell, and urban high-rise cell, respectively. The two rural cells again show a somewhat similar distribution, with a narrow peak occurring at $Bc_{0.9}$ values of 0.5 or 1 MHz and then a more spread-out second peak occurring at $Bc_{0.9}$ values around 4 or 5 MHz. Again the urban high-rise cell shows a vastly different distribution. Here, a very narrow single peak occurs in the distribution at $Bc_{0.9}$ values up to 0.5 MHz.

Figures 5.12c-5.14c present the correlation bandwidth statistics as cumulative distributions of $Bc_{0.9}$, $Bc_{0.77}$, $Bc_{0.63}$, and $Bc_{0.5}$ for the flat rural cell, hilly rural cell, and urban high-rise cell, respectively. These plots show, for all of the APDPs in a cell, the probability of correlation bandwidth being less than a given correlation bandwidth value. Note the large difference between $Bc_{0.5}$ and $Bc_{0.9}$ in all of the cells, particularly in the rural cells. As an example, in the flat rural cell, the probability of $Bc_{0.5}$ being less than 4 MHz is about 0.09 while the probability of $Bc_{0.9}$ being less than 4 MHz is about 0.7. The cumulative distributions of correlation bandwidth for the rural cells are roughly similar. For the urban high-rise cell, probabilities of correlation bandwidth being less than the abscissa are much higher than in the rural cells. The difference in the correlation bandwidth statistics between the rural cells and the urban high-rise cell tends to indicate that significantly more multipath is present in the urban high-rise environment.

6. SUMMARY AND CONCLUSIONS

This paper discusses an impulse response measurement experiment consisting of measurements taken in the 1850-1990 MHz band within three different cell environments in the Denver, Colorado, area. These environments included a flat rural cell, a hilly rural cell, and an urban high-rise cell. The measurements within each cell were made using a fixed-location receiver placed at the center of the cell and a mobile transmitter installed in a measurement van. A single binary phase-shift keyed (BPSK) PN code sequence was transmitted and a dual-channel receiver employing spatial diversity was used to receive the transmitted signal. The separation of the receive antennas was set for 15 wavelengths at the center of the 1850-1990 MHz band. In the rural cells, the receiver was located in a large measurement van and kept at a fixed location. The receive antennas were mounted on a telescoping mast 8.7 m aboveground. In the urban high-rise cell, the receiver antennas were located on the rooftop of a building 103 m aboveground in the center of the high-rise district in downtown Denver. The building height was typical for the buildings in this area. All of the measurements were made within a 5-km radius of the center of each cell. The measurements were taken using omnidirectional, vertically polarized transmit and receive antennas in all of the cells. Impulse response data were collected as the transmitter van travelled along predetermined routes within each cell. A rapid succession of 10 impulse responses was taken at intervals of approximately 0.7 s while the transmitter van was moving. Within this succession of 10 impulse responses, a time interval of 255.5 μs (5 times the PN code word duration) was used between the beginning of one impulse and the beginning of the next. This allowed for averaging of 10 impulses to reduce the noise floor. The data were analyzed to provide delay statistics; spatial diversity statistics; multipath power statistics; number of paths, path arrival time, and path power statistics; and correlation bandwidth statistics.

Three types of delay statistics were presented: maximum delay, average delay, and RMS delay spread. From these statistics, several conclusions were suggested. Slightly more multipath was seen in the hilly rural cell than in the flat rural cell. Very long delays (greater than 10 μs), while not seen often, were seen more frequently in the rural cells than in the urban high-rise cell. Although very long delays were seen more often in the rural cells, there were many more delayed signals (out to 5 or 6 μs) with higher power in the urban high-rise cell than in the rural cells. More signals with long delays (greater than 6 μs) were seen in the hilly rural cell than in the other cells.

The effects of spatial diversity were analyzed by comparing the cumulative distribution of RMS delay spread between Channel 1, Channel 2, and the diversity combination of both channels. The results of this analysis showed some, although not a large, decrease in RMS delay spread values using diversity combination. These results suggest that the wideband signals seen on each channel were indeed uncorrelated to some degree.

The multipath power statistics provided statistical information about the signal amplitude variation for every delay time for all of the APDPs in a given cell. These statistics included, as a function of delay time: average multipath power, standard deviation of multipath power, peak multipath power, and probability of multipath power exceeding a threshold. The results of these analyses agreed very well with those from the delay statistics. The urban high-rise cell had many more multipath components above threshold than the rural cells, out to 4 or 5 μs in delay. The peak (normalized) multipath power was also seen to be the highest for delays greater than 15 μs in the hilly rural cell and the lowest in the urban high-rise cell.

The goal of the presentation of the number of paths, path arrival time, and path power statistics was to provide information to assist in the development of impulse response models (primarily tapped delay models) of the radio propagation channel. The results provide an idea of the number of required taps that may be needed to model the impulse response of the radio channel (within a 100-ns resolution) in several different environments in the 1850-1990 MHz band. The results clearly showed that the urban high-rise cell would require a far greater number of taps than the rural cells for the -20 and -10 dB thresholds. It should be noted that these results, and the rest of the results of the data analyses presented in this paper, are quite dependent on the threshold level used in processing. As expected, processing with lower threshold levels (i.e., those set further below the peak in the APDP) showed more paths. Mean and standard deviation of the arrival time and path power of each individual path were presented for APDPs having a total of up to 10 paths. For a threshold of -20 dB, it was found that 10 paths can adequately represent most (89% or more) of the APDPs in each of the rural cells. In the urban high-rise cell, for a -20 dB threshold, 10 paths are not adequate to represent most of the APDPs. For a threshold of -10 dB, most (79% or more) of the APDPs in each of the cells can be adequately represented with 10 paths.

The results of the correlation bandwidth statistics show only small differences in the cumulative distributions of correlation bandwidth between the rural cells. The urban high-rise cell shows much smaller correlation bandwidth values than in the rural cells. This indicates that significantly more multipath was seen in the urban high-rise cell than in the other cells; consistent with the findings in the other forms of data analyses presented here.

Finally, it should be noted that these impulse response measurements were made with a system having a 20 MHz bandwidth. The results are expected to be different for measurements taken with systems having different bandwidths.

7. REFERENCES

[1] R.C. Dixon, *Spread Spectrum Systems*, New York: John Wiley & Sons, Inc., 1976, pp. 7.

[2] D.C. Cox, "Delay doppler characteristics of multipath propagation at 910 MHz in a suburban mobile radio environment," *IEEE Trans. on Antennas and Propagation*, AP-20, No. 5, pp. 625-635, September 1972.

[3] D.C. Cox, "Time- and frequency-domain characterizations of multipath propagation at 910 MHz in a suburban mobile-radio environment," *Radio Science*, Vol. 7, No. 12, pp. 1069-1077, December 1972.

[4] D.C. Cox and R.P. Leck, "Correlation bandwidth and delay spread multipath propagation statistics for 910 MHz urban mobile radio channels," *IEEE Trans. Communications*, COM-23, No. 11, pp. 1271-1280, November 1975.

[5] D.M.J. Devasirvatham, "Multipath time delay spread in the digital portable radio environment," *IEEE Communications Magazine*, Vol. 25, No. 6, pp. 13-21, June 1987.

[6] R.C.V. Macario, *Personal and Mobile Radio Systems,* London, U.K.: Peter Peregrinus, Ltd., 1991, pp. 31-32.

[7] CCIR, "Propagation data and prediction methods for the terrestrial land mobile service using the frequency range 30 MHz to 3 GHz," CCIR Report 567-4, International Radio Consultive Committee, International Telecommunications Union, Geneva, Switzerland, 1990.

FORM **NTIA-29**
(4-80)

U.S. DEPARTMENT OF COMMERCE
NAT'L. TELECOMMUNICATIONS AND INFORMATION ADMINISTRATION

BIBLIOGRAPHIC DATA SHEET

	1. PUBLICATION NO.	2. Gov't Accession No.	3. Recipient's Accession No.
	NTIA Report 94-309		

4. TITLE AND SUBTITLE

Impulse Response Measurements in the 1850-1990 MHz Band in Large Outdoor Cells

5. Publication Date

6. Performing Organization Code
ITS.S3

7. AUTHOR(S)
J.A. Wepman, J.R. Hoffman, L.H. Loew

9. Project/Task/Work Unit No.

8. PERFORMING ORGANIZATION NAME AND ADDRESS
Nat'l Telecommunications & Information Administration
Institute for Telecommunication Sciences
325 Broadway
Boulder, CO 80303

10. Contract/Grant No.

11. Sponsoring Organization Name and Address

12. Type of Report and Period Covered

13.

14. SUPPLEMENTARY NOTES

15. ABSTRACT *(A 200-word or less factual summary of most significant information. If document includes a significant bibliography or literature survey, mention it here.)*

Mobile impulse response measurements were taken in the 1850-1990 MHz band in three different macrocellular (cell radii of 5 km) environments: flat rural, hilly rural, and urban high-rise. Spatial diversity with a 15-wavelength separation was employed by using a dual-channel receiver. All antennas were omnidirectional and vertically polarized. The data were analyzed to provide delay statistics; spatial diversity statistics; multipath power statistics; number of paths, path arrival time, and path power statistics; and correlation bandwidth statistics. The urban high-rise cell showed more multipath components (out of 4 or 5 μs in delay) than the rural cells. Very long delays (greater than 10 μs), while not seen often, were seen more frequently in the rural cells than in the urban high-rise cell. Parameters to help design a tapped delay model of the radio channel in the different environments are given.

16. Key Words *(Alphabetical order, separated by semicolons)*

arrival time, channel model, coherence bandwidth, correlation bandwidth, impulse response, multipath, power delay profiles, RMS delay spread, spatial diversity, tapped delay model, wideband measurements.

17. AVAILABILITY STATEMENT	18. Security Class. *(This report)*	20. Number of pages
☒ UNLIMITED.	UNCLAS	49
☐ FOR OFFICIAL DISTRIBUTION.	19. Security Class. *(This page)*	21. Price:
	UNCLAS	